Torque Capacity and Crack Propagation Analysis of Fiber-reinforced Composite Hollow Transmission Shaft

A thesis Submitted to Addis Ababa Institute of Technology, School of Graduate Studies, Addis Ababa University

In partial Fulfillment of the Requirement for the Degree of

Master of Science in Mechanical Engineering

(Mechanical Design Stream)

By

Okqubamariam Leake

Advisor

Professor Eyassu Woldesenbet

August 2012

Addis Ababa University

School of Graduate Studies

Department of Mechanical Engineering

Torque Capacity and Crack Propagation Analysis of Fiber-reinforced Composite Hollow Transmission Shaft

A thesis Submitted to Addis Ababa Institute of Technology, School of Graduate Studies, Addis Ababa University

In partial Fulfillment of the Requirement for the Degree of

Master of Science in Mechanical Engineering

(Mechanical Design Stream)

By
Okqubamariam Leake

Addis Ababa Institute of Technology, AAiT

Approved by the Examining Board**:**

Dr. Daniel Tilahun	_____
Chairman	Signature
Professor Eyassu Woldesenbet	_____
Advisor	Signature
Dr. Daniel Tilahun	_____
External Examiner	Signature
Dr. Ing. Zewdu Abdi	_____
Internal Examiner	Signature

Acknowledgement

First and foremost I would like to thank the almighty God because without his blessing and wills this thesis would have been impossible. I would like to extend my utmost gratitude and thanks to my advisor, Professor Eyassu Woldesenbet, for his constant encouragement, unwavering support and valuable advice throughout the research. He has been supportive since the day I began working on the proposal of the research as I was new to composite materials. I remember he used to say something like "You should never let a problem an excuse in your work. Instead you have to fight for it in order to get what you want to achieve!" He used this expression to encourage me to solve the problem that I would probably face them in my research. Many thanks to his vast knowledge and insight in to the area of composite materials, it has helped me get through the obstacles along the way. Professor Eyassu was not only my thesis adviser for the last two years, but also a good adviser of my personality and the inspiration I have to have in my life through the rough road to finish this thesis. During the most difficult times when I was writing this thesis, he gave me the moral support and freedom I needed to move on.

I would like to express my warmest thanks to Dejen Aviation Engineering Complex, DAEC, for letting me to use the glass fiber and polyester resin to manufacture the transmission shaft and Defense Engineering College, DEC, for letting me to use the torsion testing machine.

I would like to thank Lt. Endalkachew Kebede, head of Design and Development in Dejen Aviation Engineering Complex, for his cooperative in manufacturing the specimens in filament winding shop of the company.

I also would like to thank Capt. Getu, Lt. Asegedech, Ato Solomon, Ato Fukadu and other machinists in the filament winding shop of Dejen Aviation Engineering Complex for guiding me through all the manufacturing of the glass fiber-reinforced polyester polymer composite specimens for the experiment. Thanks to Mr. Sirvalsu Reddy Kassu and Mr. Ananthrum, instructors in Defense Engineering College**,** for being my major advisors. Mr. Kassu guided me

how to model and analyze the glass fiber-reinforced polyester polymer composite transmission shaft in ANSYS software; and Mr. Ananthrum has supported me to analyze the crack propagation of the transmission shaft.

I would also like to thank Sgt. Amare Tamene, lab assistant in material testing shop of Defense Engineering College, for letting me to test and helping me in testing of the glass fiber-reinforced polyester polymer composite hollow transmission shaft on the torsional testing machine.

A special thanks goes to my brother, Hagos Birhane, for his patience to read and edit this paper and giving me a moral support throughout the duration of this thesis. I would also want to thank my friends Solomon Kiros and Weldie Dimtsu for helping me in reading and editing of this paper.

Last but not the least, I would like to thank Mokennen Abebe, PhD, department head of Center for Research and Development of Defense Engineering College, and my friends, for their unwavering support and encouragement which provided me the strength to complete this study.

Table of content

Contents **Page**

Acknowledgement i

Table of content iii

List of figures v

List of tables vii

Abstract viii

Notation ix

Chapter One 1

1. Introduction 1

1.1. Over view of the thesis 2

1.2. Objective of the thesis 4

Chapter Two 5

2. Background 5

2.1. Classification of composites 6

2.2. Composite materials manufacturing process 15

2.3. Advantage of fiber-reinforced composite materials 16

2.4. Limitation of composite materials 17

2.5. Application of composite materials 17

Chapter Three 19

3. Literature survey 19

3.1. Literature review 19

3.2. Motivation 25

Chapter Four 27

4. Design Analysis of transmission shaft 27

4.1. Working condition of the shaft 27
4.2. Manufacturing of the shaft 29
4.3. Design of torque capacity of transmission shaft 37
4.4. Torsional buckling capacity 40
4.5. Crack propagation analysis 42
Chapter Five 49
5. Finite element analysis 49
5.1. Introduction 49
5.2. Modeling the composite shaft 50
5.3. Torque capacity analysis on ANSYS 54
5.4. Crack propagation analysis on ANSYS 57
Chapter Six 61
6. Solution Techniques 61
6.1. Introduction 61
6.2. Testing 61
Chapter Seven 66
7. Result and Discussion 66
Chapter Eight 73
8. Conclusions and Recommendations 73
8.1. Conclusions 73
8.2. Recommendations for future researches 75
References 76
Appendix-A 79
Appendix-B 80

List of figures

Figure 2-1: - Fiber-reinforced composites (a) straight and continuous fibers (b) discontinuous or particulate or chopped fibers 8

Figure 2-2: - Classification of composite material 9

Figure 4-1: - H260L model helicopter 27

Figure 4-2: - Manufacturing of the hollow transmission shaft 30

Figure 4-3: - The local and global coordinate of the transmission shaft 34

Figure 4-4: - Global coordinate of the transmission shaft 36

Figure 4-5: - Mode-I, opening mode of loading 42

Figure 4-6: - Mode-II, sliding mode of loading 42

Figure 4-7: - Mode-III, tearing mode of loading 43

Figure 4-8: - Transmission shaft subjected to torque 44

Figure 4-9: - Through-thickness central crack 45

Figure 4-10: - Crack tip polar coordinate 47

Figure 5-1: - Solid46 DOF and element type 50

Figure 5-2: - The stacking sequence for the transmission shaft 55

Figure 5-3: - The zoomed 3D model of the transmission shaft 55

Figure 5-4: - Zoomed Meshed model of the transmission shaft 56

Figure 5-5: - Von Misses stress of the transmission shaft 57

Figure 5-6: - Meshed quarter part of plate with central crack 58

Figure 5-7: - Deformation of the central symmetry crack 59

Figure 5-8: - Stress intensity factor from ANSYS 59

Figure 5-9: - Von Misses stress of the cracked plate 60

Figure 6-1: - Torsion testing machine 63

Figure 6-2: - Glass fiber-reinforced hollow circular shaft specimens 63

Figure 6-3: - Assembled specimen, end clamp and hose clip together 64

Figure 6-4: - Torsion testing machine with specimen 65

Figure 7-1: - Torque versus stress $[+45/90/-45]_2$, $[+45/90/-45]$ and $[+45/-45]$ 67

Figure 7-2: - Torque vs twisting angle $[+45/90/-45]_2$, $[+45/90/-45]$ and $[+45/-45]$ 68

Figure 7-3: - Torque versus twisting angle for $[90]_2$, $[90]_4$ and $[90]_6$ 69

Figure 7-4: - Torque versus twisting angle for $[\pm 45]$, $[\pm 45]_2$ and $[\pm 45]_3$ 69

Figure 7-5: - Torque versus twisting angle for $[+45/90]$ and $[\pm 45/90]_2$ 70

Figure 7-6: - Torque versus twisting angle for $[\pm 45]$, $[90]_2$ and $[+45/90]$ 70

Figure 7-7: - Torque versus twisting angle for $[\pm 45]_3$, $[90]_6$ and $[\pm 45/90]_2$ 71

Figure 7-8: - Comparison between the (a) ANSYS and (b) experimental results 72

List of tables

Table 4-1: - Mechanical and physical properties of carbon steel 6061 28

Table 4-2: - Some typical properties of polyester resin 31

Table 4-3: - Typical property of glass fiber..... 32

Table 4-4: - Engineering constants of the composite transmission shaft 34

Table 4-5: - Engineering constants along the global coordinate 36

Table 4-6: - The mechanical properties for the glass fiber-reinforced composite..... 37

Table 4-7: - Stress near the crack tip of a through-thickness central crack..... 46

Table 6-1: - Specimens of different size and angle of orientation 64

Abstract

The main purpose of this thesis is to investigate torque capacity and crack propagation resistance of glass fiber-reinforced polyester polymer composite material. This has been done in order to use this composite material for the transmission shaft of Hidasie helicopter (model of H260L helicopter) of Dejen Aviation Engineering Complex, DAEC.

A glass fiber-reinforced polyester polymer composite hollow transmission shaft is manufactured in filament winding machine by winding of impregnated fiber around a mandrel layer by layer with different orientation angle and stacking sequence. The elastic engineering constants of composite transmission shaft are also determined using the Classic Laminate Theory, CLT. An experiment on the torsion testing machine reveals that the torque capacity of the hollow transmission shaft increases with increasing its thickness. It also shows that the $[+45^0/-45^0/\ 90^0]_{2s}$ stacking sequence with six number of layers is capable to carry the torque which is applied to the transmission shaft of the helicopter. Analytical analysis on its torque capacity, crack propagation resistance, and torsional buckling capacity has been also made.

Linear Elastic Fracture Mechanics, LEFM is used to analyze its crack propagation by taking a through-thickness central crack. The stress at the crack tip is analyzed hence the glass fiber-reinforced polyester polymer composite transmission shaft has good resistance to crack propagation. ANSYS finite element software is used to perform the numerical analysis for the transmission shaft. Full scale transmission shaft specimen is analyzed. The results show that the static torque capacity is significantly affected by changing orientation angle, stacking sequences and number of layers.

A Good agreement is obtained among the finite element predictions and experimental and analytical results. And finally, few recommendations are also made for future study.

Notation

FRP- Fiber reinforced plastics

DAEC-Dejen Aviation Engineering Complex

DEC- Defense Engineering College

FE – Finite Element

FEA – Finite Element Analysis

FEM – Finite Element Method

DOF – Degree of Freedom

LEFM – Linear Elastic Fracture Mechanics

SIF – Stress Intensity Factor

PMC – Polymer-Matrix Composite

MMC – Metal-Matrix Composite

CMC – Ceramic-Matrix Composite

CLT – Classic Laminate Theory

d_0 - Outside diameter

d_i - Inside diameter

t - Thickness

α - Fiber orientation angle

L - Length

φ - Twisting angle

T - Torque

G - Shear modulus of the steel shaft

d - Diameter

ρ - Mass density of the shaft

V - Volume

V_f - Volume of fiber

V_m - Volume of matrix

V_c - Volume of composite

v_f - Volume fraction of fiber

v_m - Volume fraction of matrix

w_f - Weight fraction of fiber

w_m - Weight fraction of matrix

W_f - Weight of fiber

W_m - Weight of matrix

W_c - Weight of composite

ρ_f - Density of fiber

ρ_m - Density of matrix

E_1 - Longitudinal modulus of Elasticity composite shaft

E_2 - Transverse modulus of Elasticity composite shaft

G_{12} - Shear modulus of composite shaft

v_{12} - Poison's ratio of composite shaft

$[Q]_{Esks}$ - Plies rigidity in ply coordinate

$[Q]_{lamks}$ - Plies rigidity in global coordinate

$[A]$ - Laminate rigidity matrix

$[a]$ - Laminate compliance matrix

t_k - Thickness of a single ply

t_{lam} - Thickness of a laminate

P - Power

ω - Angular velocity

f - Frequency

ϕ - Angle of twisting per unit length

J - Polar moment of inertia

r - Radius of the shaft

τ - Shear stress

γ - Shear strain

m - Mass

u - Displacement in x-direction

v - Displacement in y-direction

w - Displacement in z-direction

τ_{cr} - Critical shear stress

T_{cr} - Critical torsional buckling

σ_{ij}^{I} - Stress in opening mode of fracture

σ_{ij}^{II} - Stress in sliding mode of fracture

σ_{ij}^{III} - Stress in tearing mode of fracture

b - Width of the small area taken for crack propagation analysis

a - Half crack size

σ - Remote tensile stress

K_I - Stress intensity factor for opening mode of loading

K_{II} - Stress intensity factor for sliding mode of loading

θ - Polar angular coordinate at the crack tip

Chapter One

1. Introduction

Conventional aerostatic shafts, usually made of steel, are not only heavy weight with little damping properties, but are also susceptible to whirling vibration at high rotational speed. Recently, high precision and high speed aerostatic shafts have been widely used because of low friction and low heat generation [13]. However, these aerostatic shafts have low stiffness and poor damping properties due to low viscosity of air, and consequently have a low starting value of whirl vibration if heavy metallic shafts are employed. These problems associated with metallic shafts can be overcome by shafts made from fiber reinforced composite materials particularly in this research from fiber glass-polyester reinforced composite material.

It is known that during operation, rotating shafts are subjected to degenerative effects which may cause initiation of structural defects such as crack and crack-like which finally leads to the catastrophic failure or breakdown of the shaft. Thus, it is important to design for crack propagation and vibration analysis of the shaft. In addition, inspection in the quality assurance of the manufactured shaft is well understood even while the shaft is in operation.

Several methods, such as destructive and non-destructive tests, can be used to monitor the crack and vibration condition of the shaft. It is clear that new reliable and inexpensive method to monitor structural defects of the shaft such as cracks and crack-like should be explored. Cracks and other structural defects in the shaft will influence its dynamical behavior and change its stiffness and damping properties. Consequently, the natural frequencies and mode shapes of the shaft contain information about the location and dimensions of the crack.

Vibration analysis, which can be used to detect structural defects of the shaft such as crack and crack-like, of any structure offers an effective, inexpensive and fast means of non-destructive testing. What types of changes occur in the vibration characteristics of the shaft, how changes

can be detected and how the condition of the shaft is interpreted has been the topic of several research studies in the past and reviewed by many researchers [3].

Nowadays, the interest of using composite materials for structural purposes in many branch of engineering such as aircraft, turbo machinery, and power plants is increasing. It is due to the reason that composite materials have good characteristics such as high strength-to-weight and stiffness-to-weight ratio, good damping capacity and better resistance to fatigue and crack propagation [9] as compared to monolithic materials such as metals; individuals are interested in composite materials. So rotating transmission shaft of the aircraft or any power plant can be made from fiber-reinforced composite materials. This may show us that composite transmission shaft of a helicopter is one of the potential applications of composite materials.

1.1. Over view of the thesis

Application of composite materials in many engineering designs and products such as automobile, aircrafts, turbo machineries, marine, trains, constructions and machine components of power plants has increased dramatically. Nowadays most of components of aircrafts such as helicopter; and marine such as boat are made from composite materials. Therefore, it is important to take care in designing and material selection for the components of the aircrafts and marines. Otherwise, the consequence is very costly and may also cause catastrophic failure in terms of human life and property damage.

Aircrafts and marines are designed by optimizing their own weight (dead load) and the capacity they could carry. It is necessary for an aircraft to have light weight for the sake of fuel consumption as well. The fuel consumption of an aircraft is proportional to the weight it carries. Currently, most aircraft manufacturing companies are trying to increase the carrying capacity of an aircraft by reducing its own weight. At the same time, they are analyzing the strength of each component of the aircraft in order to cop up with the weight that it is supposed to carry.

Fiber-reinforced composite materials are suitable for the above mentioned functions. Fiber-reinforced composite materials are uniquely useful because the use of long fibers results in a material which has a higher strength-to-mass and stiffness-to-mass ratio than any other material system at moderate temperature. It is true that composite materials have unique mechanical property due to fiber orientations to a given geometry, applied load and environmental system of the structure. Most of the time short fiber composites are used in high production and low cost systems. It is not only due to weight and stiffness but also due to the use of fibers as reinforcement that makes the composite materials competitive and superior to the plastics and metal alternatives [16].

Dejen Aviation Engineering Complex, DAEC, a company in Debrezeyt, tried to have a H260L model helicopter with light-weight by manufacturing all its parts from composite material. In doing so the company tried to make the helicopter carries as much weight as it used to carries and they call it Hidasie helicopter. Most of its components are manufactured from glass fiber-reinforced polyester polymer composite material by reverse engineering and assembled it. However, there are some components of the helicopter which need analysis and simulations before manufacturing by reverse engineering. One of these components is the transmission shaft, which transmits torque from the main gear-box to the intermediate gear-box.

The transmission shaft of the H260L model helicopter is made from 6061 carbon steel. However, DAEC wants to change it by glass fiber-reinforced polyester polymer composite material. Even if using fiber-reinforced composite materials have an advantage in reducing the weight, increase in strength and resistance in crack propagation, experiment has to be performed for the glass fiber-reinforced polyester polymer composite transmission shaft of the helicopter. Since the transmission shaft is subjected to torque, it is necessary to design for torsional capacity and analyze the crack propagation in case a defect might appear during manufacturing or operation. It is also necessary to test the glass fiber-reinforced polyester polymer composite transmission shaft experimentally for torsion load on torsion testing machine.

1.2. Objective of the thesis

The general objective of this thesis is to analyze and simulate crack propagation and torque capacity of fiber-reinforced composite transmission shaft for Hidasie helicopter. In addition, an experiment on the torque capacity of the transmission shaft is going to be performed on torsion testing machine in order to verify the analytical results.

The specific objectives of this thesis include:

- To change and manufacture the material of the transmission shaft from 6061 carbon steel to glass fiber-reinforced polyester polymer matrix composite material.
- To model and analyze the glass fiber-reinforced composite hollow transmission shaft on commercial structural analysis software, ANSYS.
- To study and identify the torque capacity of the fiber-reinforced composite transmission shaft with respect to its thickness, orientation angle and stacking sequence.
- To study and identify the nature of crack propagation with respect to its crack location and crack direction of the fiber-reinforced composite transmission shaft.

These objectives will be achieved by employing the following procedures:

- Modeling a hollow transmission shaft with a structural member on ANSYS software.
- Modeling the crack on the hollow transmission shaft in terms of the type of crack and where crack propagates in reality.
- Apply the finite element software to analyze torque capacity, torsional buckling, and crack propagation on ANSYS.
- Analyzing the torque capacity, torsional buckling capacity and crack propagation analytically.
- Performing an experiment on torsion testing machine for the torque capacity of the hollow transmission shaft.
- Discuss and compare the results that are obtained from ANSYS software, analytical analysis and experiment.

2. Background

Composite materials emerged in the middle of the 20th century as a promising class of engineering materials providing new prospects for modern technology. It is a macroscopic combination of two or more distinct materials with a recognizable interface between them. The constituents retain their identities in the composite; that is, they do not dissolve or otherwise merge completely into each other, although they act in concert [27].

In general, any material consisting of two or more constituents with different properties and distinct boundaries between the constituents can be referred to as a composite material [17]. In addition to the above definition, three other criteria should normally be satisfied in order for a material to be called a composite material. These criteria are:

i. Both constituents have to be present in reasonable proportions.
ii. The constituent phases should have distinctly different properties, such that the composite's properties are noticeably different from the properties of the constituents.
iii. A synthetic composite is usually produced by deliberately mixing and combining the constituents by various means.

The above definition would encompass bricks, concrete, wood, bone, as well as modern synthetic composites such as fiber-reinforced plastics, FRP. The fiber-reinforced plastics have become increasingly important over the past 50 years, and are now the first choice for fabricating structures where low weight in combination with high strength and stiffness are required [18].

Composite materials are completely different from alloy materials. There are two main differences between composite and alloy materials. First, the constituent materials in composite are insoluble in each other, whereas soluble in each other in alloys. Second, the individual

constituents retain their properties in the case of composites, whereas form a new material which has different properties from their constituents in alloys [12].

2.1. Classification of composites

It is known that composite materials have two or more chemically distinct constituents on a microscopic scale and separated by a distinct interface. It is important to be able to specify these constituents. The constituent that is continuous and often, but not always, present in the greater quantity in the composite is the matrix. It is the properties of this matrix that are improved upon when incorporating another constituent to produce a composite. A composite may have a ceramic, metallic or polymeric matrix. So based on their matrix, composite materials can be classified as [17]:

- Polymer-matrix composite (PMC)
- Metal-matrix composite (MMC)
- Ceramic-matrix composite (CMC)

The mechanical properties of these three classes of material differ considerably. As a generalization, polymers have low strength and Young's modulus; ceramics are strong, stiff and brittle; and metals have intermediate strength and modulus, together with good ductility i.e. they are not brittle [18].

Technologically, polymer matrices composite are the most important composites. These composite materials can be classified based on different methods. For instance, they can be classified into two according to the way their components are mixed and oriented. These are filled composite materials and fiber reinforced composite materials [1].

- **Filled composite materials**: - the main feature of these materials is the existence of some basic or matrix materials whose properties are improved by filling it with some particles. Usually the matrix volume fraction of these materials is more than 50%.
- **Fiber-reinforced composite materials**: - they are also known as advanced composites. The basic components of these materials are long and thin fibers possessing high

strength and stiffness. The fibers in these materials are bounded with matrix whose volume fraction is usually less than 50%.

The second constituent of the composite material is known to as the reinforcement. This constituent enhances or reinforces the mechanical properties of the matrix. Although there are some exceptions, in most cases the reinforcement is harder, stronger and stiffer than the matrix. The geometry of the reinforcing is one of the major parameters in determining the effectiveness of the reinforcement; in other words, the mechanical properties of composites are a function of the shape and dimensions of the reinforcement. Figure 2-2 represents a commonly employed classification of composite materials based on their reinforcement [17].

Based on their reinforcement, it is usually described that composite materials as being either fibrous or particulate.

i. **Particulate composites**: - They have dimensions that are approximately equal in all directions. The shape of the reinforcing particles may be spherical, cubic, platelet or any regular or irregular geometry. The arrangement of reinforcement in the particulate composites may be random or with a preferred orientation. As shown in figure 2-2 this characteristic is also used as a part of the classification scheme.

ii. **Fibrous composites**: - The reinforcement they use is characterized by its length being much greater than its cross-section dimensions. However, the ratio of length to a cross-section dimension, known as the aspect ratio, can vary considerably. In single-layer composites long fibers with high aspect ratios give what are called continuous fiber-reinforced composites, whereas discontinuous fiber composites are fabricated using short fibers of low aspect ratio [17].

The reinforcing fibers may be continuous or discontinuous, as shown in Figure 2-1 (a) and (b). The latter can be in the form of short fibers, whiskers, or particulates. Longitudinal fibers are used in both epoxy and metal-matrix composites. Whiskers and particulates are more often found in metal-matrix composites. The main advantage of discontinuously

reinforced composites is that they can be fabricated using processing techniques similar to those commonly used for unreinforced matrix materials, which makes them more cost effective [27]. In addition, discontinuously reinforced composites have relatively more isotropic properties than continuously reinforced composites, due to the lower aspect ratio and more random orientation of the reinforcements.

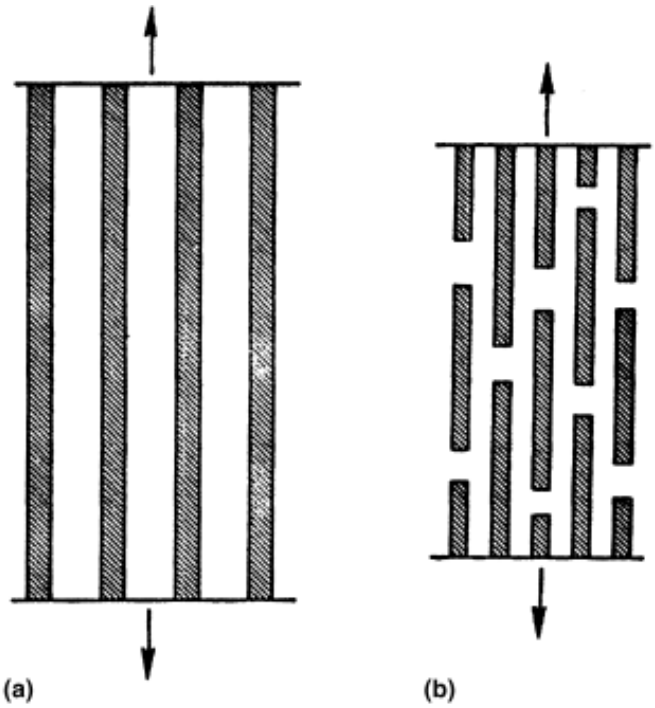

Figure 2-1: - Fiber-reinforced composites (a) straight and continuous fibers (b) discontinuous or particulate or chopped fibers

Composite materials can be classified based on the fiber they have in their composition. The fibers they have may be continuous or discontinuous. This classification is shown in figure 2-2.

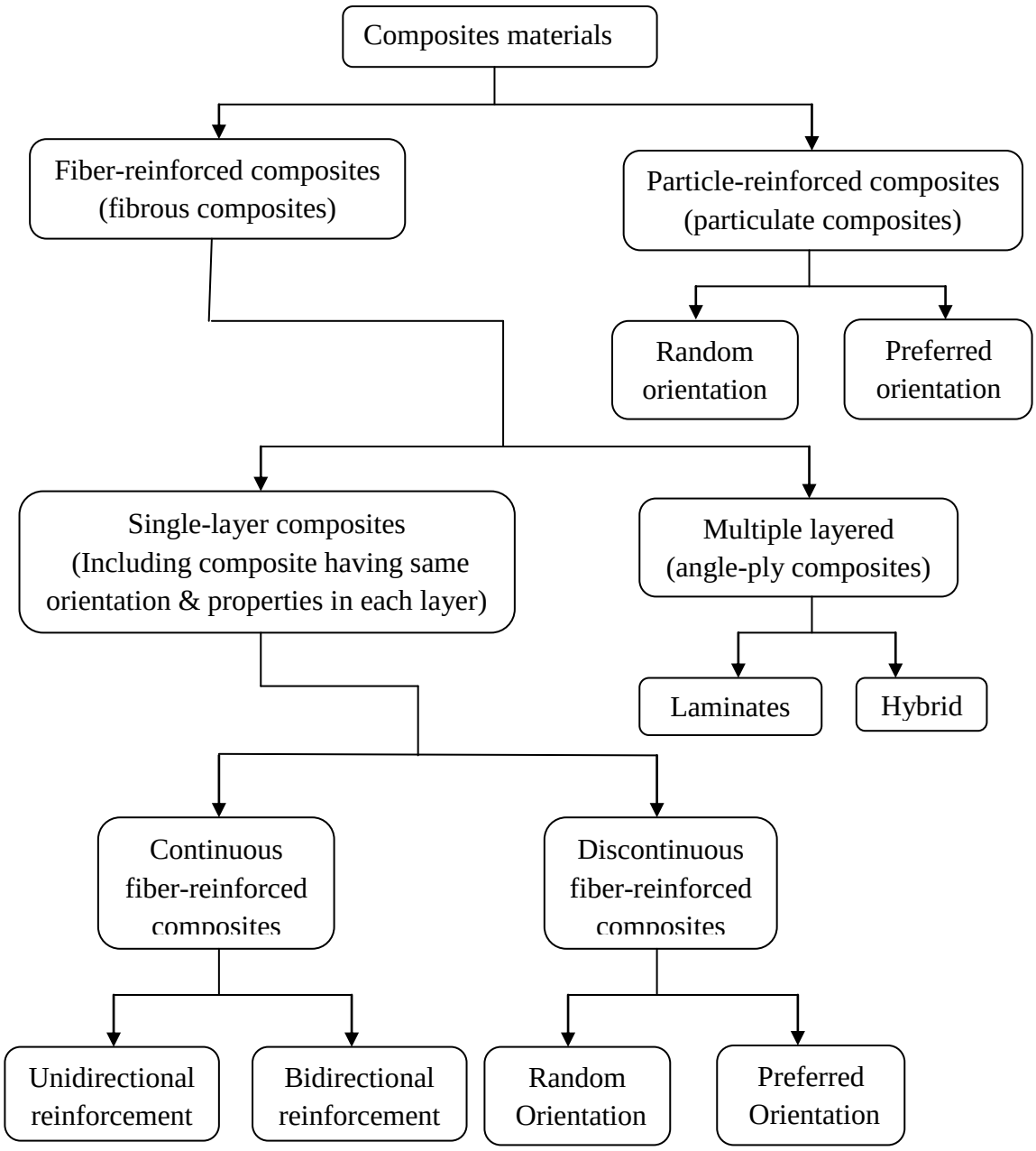

Figure 2-2: - Classification of composite material

The orientation of the discontinuous fibers may be random or preferred. The frequently encountered preferred orientation in the case of a continuous fiber composite is termed unidirectional and the corresponding random situation can be approximated by bidirectional woven reinforcement.

Multilayered composites are another category and commonly used form of fiber-reinforced composites. These are classified as either laminates or hybrids. Laminates are sheet constructions which are made by stacking layers. They are also called plies and usually are unidirectional in a specified sequence. The layers are often in the form of prepreg (fibers pre-impregnated with partly cured resin) which are consolidated in an autoclave.

A laminate may have between 4 and 400 layers and the fiber orientation changes from layer to layer in a regular manner through the thickness of the laminate.

Hybrids are composites with mixed fibers and are becoming commonplace. The fibers may be mixed within a ply or layer by layer. So these composites are designed to benefit from the different properties of the fibers employed. For example, a mixture of glass and carbon fibers incorporated into a polymer matrix gives a relatively inexpensive composite, owing to the low cost of glass fibers, but with mechanical properties enhanced by the excellent stiffness of carbon.

In this research a fiber-reinforced composite material is used. Fibers and matrices are the constituent of the fiber-reinforced composite material.

2.1.1. Fiber: - As it has been explained that the reinforcement for a composite may be fibrous or particulate. A wide range of both these forms of reinforcement is available for use in the production of composite materials but most of the major developments in recent times have been in the area of fibrous reinforcement. The

important aspect in the design of fiber composite materials is to find or to make a fiber material of high elastic modulus and strength. In addition, the fiber should have preferably low density so as to arrange the fibers in a suitable manner to give useful engineering properties to the final product.

The manufacture of the fibers involves a number of processing steps and variability of properties from one fiber to another, even when made by the same process. The microstructure and properties of fibers of the same material made by different processes can differ even more markedly. Furthermore, the high tensile strength of freshly made fibers is normally reduced by surface damage caused during subsequent handling and storage. Finally, any variation in size leads to a range of strength values [18]. There are different types of fibers such as glass, boron, carbon, quartz, aramid and basalt.

- **Glass fiber*:* -** There are many groups of glass fibers such as silica, oxynitride, phosphate and halide glass fibers. Currently, Silica glass fibers are the only important glass fibers from the point of view of composite material technology. However, even within this group of glasses the composition and properties vary considerably. The most commonly used glass fiber is E-glass, the E being an abbreviation for electrical [18].

  Continuous glass fibers are made by pulling molten glass at a temperature about 1300 ^{0}C through 0.8 to 3 mm diameter dies and further high speed stretching to a diameter of 3 to 19 μm. Usually, glass fibers have solid circular cross-section. The typical mechanical characteristics and density of these glass fibers are: 3100 to 5000 MPa ultimate tensile strength, 72 to 95 GPa modulus of elasticity and 2.4 to 2.6 specific gravity. The important properties of glass fibers as components of reinforced materials for engineering applications are their high strength (which is maintained in humid environments but degrades under

elevated temperatures), relatively low stiffness (about 40% of the stiffness of steel), high chemical and biological resistance, and low cost. Being actually elements of monolithic glass, the fibers do not absorb water and do not change their dimensions in water. For the same reason, they are brittle and sensitive to surface damage.

- **Carbon fiber:** - These fibers are produced by many companies. The world production capacity of carbon fiber exceeds 20,000 tonnes [18]. In spite of this large production capacity, carbon fibers are still relatively expensive. Nevertheless the usage for carbon fibers continues to increase, and many companies have recently increased their production capacity.

  The structure and properties of these fibers vary considerably and new fibers are always under test. For example two recent introductions are hollow fibers and coiled fibers. The former are designed to impart better impact toughness to carbon-reinforced polymers, whereas the latter are capable of extending many times their original length without loss of elasticity.

  Carbon has two well-known crystalline forms. These are diamond and graphite. It also exists in quasi-crystalline and glassy states. As far as fiber technology is concerned, graphite is the most important structural form of carbon.

  An unusual characteristic of carbon fibers is their very low, or even slightly negative, coefficient of longitudinal expansion. As for other properties, the coefficient of thermal expansion depends on the fabrication route and hence degree of graphitization and crystal orientation [18].

2.1.2. Matrix*:* - In order to utilize the high strength and stiffness of fibers in fiber reinforced composite materials, suitable for engineering applications; the fibers are

bounded with a matrix whose strength and stiffness is naturally much lower than fibers. Matrix materials provide the final shape of the composite structure and govern the manufacturing process. Typical matrices are made from polymeric, metal, carbon, and ceramic materials [17]. Polymeric matrix materials are divided into two. These are thermoset and thermoplastic polymers.

❖ **Thermoset polymers*:*** - They are most widely used matrices for fiber reinforced composite materials. These are polyester, epoxy, polyamide and other resins. A thermoset matrix cannot be reset, dissolved, or melted. Heating of a thermoset materials results first in degradation of its strength and stiffness and then in thermal destruction [17].

❖ **Thermoplastic polymers*:*** - These matrices include polysulfone, polyetheretherketone, polyphenylene sulfide and others. These materials don't require any curing reaction and melt under heating and convert to a solid state under cooling. The possibility to re-melt and dissolve thermoplastic matrices allows us to reshape composite parts forming them under heating and simplifies their recycling [17].

2.1.3. Filler*:* - The term "fillers" is often associated with extenders added to a matrix to reduce the total cost of the combination. However, fillers in glass fiber-reinforced composites are predominately added to engineering-specific properties with relatively inexpensive materials. The predominant use of fillers is with thermosetting resins, although some filler types are used in thermoplastic compounding. Fillers are used to impart special characteristics in processing or in the composite application. A wide range of both inorganic and organic fillers are available. Inorganic fillers are most widely used in conjunction with unsaturated polyester resins.

The ideal filler material for thermosetting resins should meet requirements such as good dispersibility, suspension stability, low density, light color, low moisture content, negligible influence on cure properties, controlled particle size distribution, heat resistance, chemical resistance and low cost [19].

The optimal combination of fiber and matrix properties should satisfy a set of operational and manufacturing requirements that are sometimes of a contradictory in nature, and have not been completely met yet in existing composites.

First of all, the stiffness of the matrix should correspond to the stiffness of the fibers and be sufficient to provide uniform loading of fibers. The fibers are usually characterized by relatively high scatter in strength that may be increased due to damage of the fibers caused by the processing equipment. Naturally, fracture of the weakest or damaged fiber should not result in material failure. Instead, the matrix should evenly redistribute the load from the broken fiber to the adjacent ones and then load the broken fiber at a distance from the cross section at which it failed. The higher the matrix stiffness, the smaller is this distance, and less is the influence of damaged fibers on material strength and stiffness. But on the other hand, to provide material integrity up to the failure of the fibers, the matrix material should possess high compliance.

However, matrix properties, even though being optimal for the corresponding fibers, do not manifest in the composite materials if the adhesion (the strength of fiber-matrix interface bonding) is not high enough. High adhesion between fibers and matrices, providing material integrity up to the failure of the fibers, is a necessary condition for high-performance composites. Proper adhesion can be reached for properly selected combinations of fiber and matrix materials under some additional conditions [17].

2.2. Composite materials manufacturing process

The combination of fiber and matrix to form a composite structure configuration is achieved through an appropriate fabrication process. There are different types of fabrication process of composite materials. It should be noted that each of these fabrication process has certain inherent advantages associated with production, design and economic circumstances. The fabrication processes used are powder metallurgy, pressure and bonding, liquid infiltration, plating, filament winding and others [16].

2.2.1. Powder metallurgy*:* - The reinforcing materials used for this fabrication technique are whiskers or chopped fibers. In this technique the aligned or unaligned fiber materials are mixed with an appropriate power matrix introduced into a die pressed under high pressure. Finally, a composite of the matrix and chopped fiber is formed. This technique has disadvantage because it may produce damaged fiber during the pressing operation if the powder size is greater than the mean diameter of the fiber.

2.2.2. Pressure and roll bonding*:* - Layers of sheet of matrix material and aligned fibers are placed alternatively one on top of another and then heated the combination to high temperature. Finally, either it is pressed together or rolled to form the composite material. The shortcoming of this technique is the fiber-matrix interface may react due to the long time associated pressing operation.

2.2.3. Liquid infiltration*:* - In general two techniques are commonly used for this type of processing. The first technique is to introduce the molten matrix into the aligned and packed fibers using either gravity or vacuum suction. On the reverse, the second technique is to introduce the fibers into the molten matrix. The second technique depends upon the wetting of the matrix/fibers system. If the matrix/fibers system has effective wetting, the matrix can be infiltrated and solidified fast. Whereas, if the matrix/fibers system has less effective wetting , vacuum drawing, with matrix drawn against the aligned fibers, may be necessary.

A major problem with this technique is the inherent reaction produced in the interfacial zone between fiber and matrix due to the thermal environment necessary for this composite material to occur.

2.2.4. Filament winding*:* - This is one of the earliest fabrication process used for producing continuous filament composites. This process can be used to form controlled composites in two optional formats. In the first, the filaments are pre-impregnated by passing them through a suitable matrix, while the second option requires winding the fibers on to a mandrel and impregnating the total filament assembly. When sufficient numbers of layers of fibers have been appropriately laid down, the impregnated windings are cured.

Filament winding uses continuous reinforcement to achieve efficient utilization of fiber strength. Roving or single strand are fed through a bath of resin and wound onto a suitably designed mandrel. Pre-impregnated roving can also be used. Special lathes laid down continuous glass fibers in a predetermined pattern to give maximum strength in the directions required. When the layers have been applied, the wound mandrel is cured at room temperature or in an oven [16].

2.3. Advantage of fiber-reinforced composite materials

Fiber-reinforced composite materials offer many advantages compared to conventional materials such as metals [12]. The advantages are:

- High strength to weight ratio
- High stiffness to weight ratio
- High impact resistance
- Better fatigue resistance
- Improved corrosion resistance
- Good thermal conductivity

- Low coefficient of thermal expansion. As a result, composite structures may exhibit a better dimensional stability over a wide temperature rang.
- High damping capacity

2.4. Limitation of composite materials

Like all other engineering materials composite materials have limitations. These limitations are [12]:

- Mechanical characterization of a composite structure is more complex than that of a metallic structure
- The design of fiber reinforced structure is difficult compared to a metallic structure, mainly due to the difference in properties in directions
- The fabrication cost of composites is high
- Rework and repairing are difficult
- They do not have high combination of strength and fracture toughness as compared to metals
- They do not necessarily give higher performance in all properties used for material selection

2.5. Application of composite materials

The common applications of composite materials are extending day to day. Nowadays, they are used in medical application too. The other fields of applications are [12]:

- **Automotive*:-*** Drive shafts, clutch plates, engine blocks, push rods, frames, valve guides, automotive racing brakes, filament-wound fuel tanks, fiber glass/epoxy leaf springs for heavy trunks and trails, rocker arm covers, suspension arms and bearings for steering system, bumpers, body panels and doors
- **Aircraft: -** Drive shafts, rudders, elevators, bearings, landing gear doors, panels and floorings of airplanes etc.
- **Space*: -*** Payload bay doors, remote manipulator arm, high gain antenna, antenna ribs and struts etc.

- **Marine*:* -** Propeller vanes, fans & blowers, gear cases, valves & condenser shells.
- **Chemical Industries*:* -** Composite vessels for liquid natural gas for alternative fuel vehicle, racked bottles for fire service, mountain climbing, underground storage tanks, ducts and stacks etc.
- **Electrical &Electronics*:* -** Structures for overhead transmission lines for railways, power line insulators, lighting poles, fiber optics, tensile members etc.
- **Sport Goods*:* -** Tennis rackets, golf club shafts, finishing rods, bicycle framework, hockey sticks, surfboards, helmets and others.

3. Literature survey

3.1. Literature review

The application and using of composite materials in aircraft for aviation and spaceflight became suitable in the recent years. This is because they have high strength-to-weight and stiffness-to-weight ratio, better resistance to fatigue and ability to redistribute the load.

Due to the wide use of composite materials in a variety structure of aircraft as well as their substantial benefits and great promise for future application, the dynamic behavior of composite materials in a structure have received a widespread attention and have been investigated extensively by many researchers. Some of the researchers' out puts which are related to the objective of this thesis are discussed below.

Murat K. [3] investigated the effect of cracks on dynamical characteristics of a cantilever composite beam, made of graphite fiber-reinforced polyamide. He used the finite element and component mode synthesis methods to model the problem. He analyzed the reduction of stiffness of the cantilever beam by the fracture mechanics theory as the inverse of the compliance matrix was calculated with proper stress intensity factor and energy release rate expression. He analyzed also the effect of the location and depth of the cracks, and the volume fraction and orientation of the fibers on the natural frequencies and mode shapes of the beam with transverse non-propagating open cracks. He also demonstrated the effect of the slenderness ratio on the natural frequency and natural bending mode shape. He calculated and plotted the first, second and third natural bending mode shape as a function of crack depth ratio for different slenderness ratio and crack location.

Murat K. and M. Arif [4] also used a numerical technique applicable for analyses of free vibration analysis of uniform and stepped cracked beam with circular cross section. The

numerical technique they used was a finite element and component mode synthesis method. The component mode synthesis technique accompanied by the finite element method is essential to change a non-linear problem into linear subsystems by detaching the beam into part from cracked section. They joined the substructures by using the flexibility matrices taking into account the interaction forces derived by virtue of fracture mechanics theory as the inverse of the compliance matrix found with appropriate stress intensity factors and strain energy release rate expressions. They tried to show the natural frequencies for cracked uniform beams are lower as compared to non-cracked uniform beams. In their study using this numerical technique, they addressed the effect of the location and depth of the cracks on the natural frequencies and mode shapes of the uniform, stepped and two-step cracked beams with circular cross section separately. The research of Murat and M. Arif was limited only to the vibration analysis of beams with non-propagating open cracks which has circular cross section. In fact, there are also beams with effect of crack breathe that propagate with applied load and beams with other cross sections.

Li Jun, *et al*, [5] introduced dynamic stiffness method for analyzing the free vibration and buckling behaviors of axially loaded laminated composite beams. In the formulation they included the influence of axial force, shear deformation, rotary inertia and Poisson effect. They established the dynamic stiffness matrix directly by solving the governing differential equations of motion of laminated beam. They demonstrated the effect of axial force and boundary condition on the buckling loads, natural frequencies and mode shapes of the laminated beams. They also strongly recommended that for the lower modes the axial force should be incurred; if it did not a substantial error would be encountered.

S. K. Bhaumik, *et al*, [6] studied the cause of fatigue failure of a hollow power transmission shaft in operation. They investigated the crack of the transmission shaft due to the leakage of oil in operation. The crack was through the thickness and had propagated in a helical manner. They revealed that the crack had propagated circumferentially covering about ¾ of the shaft periphery by fluorescent dye penetrator inspection. They cleaned the fracture surface of the

cracked hollow power transmission shaft with acetone and observed under a stereo-binocular microscope to determine the fracture origin. It was found that the fracture origin coincided with one of the edges of the keyway. Finally, they concluded that the cause of the failure of the transmission shaft at edge of the keyway was due to fatigue. The fatigue crack has initiated because of stress concentrations resulting from combined effect of rough machining and inadequate fillet radius at the keyway end edges.

H. S. Kim and D. G. Lee, [7] designed one-piece hybrid drive shaft composed of aluminum and carbon/epoxy composite for a rear wheel drive automobile. They joined an aluminum yoke by press fit joining method to the hybrid composite shaft. In press fit joining method, they used a steel ring which has many small teeth to increase reliability and reduce manufacturing cost. They devised an optimal design method to obtain high strength of the press fit joint with respect to number and shape of the steel teeth. The average shear strength between the hybrid tube and the steel ring was realized to be 75MPa which was almost 3.5 times higher than that of the adhesively joint. Finally, they manufactured a prototype for one-piece automotive hybrid aluminum/composite drive shaft and tested it. In designing the one-piece automotive hybrid aluminum/composite drive shaft, they got a mass 6.3Kg, which was only 50% of the conventional two-piece steel drive shaft. The hybrid composite shaft they developed satisfies all the design requirements such as static torque capability and fundamental natural frequency.

Y. A. Khalid, *et al*, [8] carried out an experiment and analysis on bending fatigue analysis of aluminum/composite drive shafts. They used glass fiber with matrix of epoxy resin and hardener to construct the external composite layer needed for the aluminum/composite drive shafts. The hybrid shafts they used in the experiment were fabricated using filament winding technique. They conducted an experiment on four different cases. The four cases were studied using aluminum tube wounded by different number of layers of composite materials and different stacking sequence or fiber orientation angles. The four cases of composite materials, they fabricated for the experiment based on the stacking sequence and fiber orientation angle were $[\pm 45]_{nT}$, $[90]_{nT}$, $[90/90/+45/-45]_T$ and $[90/\pm 45/90]_T$. They identified the failure mode of

all the hybrid drive shafts by performing experimental test on all cases. The tests were carried out by fixing the speed of the bending fatigue machine at 200 rpm and using different bending loads for each specimen starting from 50 to 250 N. Their macroscopic level testing indicated that the cracks were initiating in the zones free of fibers or in the outer skin of resin and increase with increasing number of cycles until the failure of the specimen. They also noticed that there was no fiber breakage from the rotating bending fatigue test. The result they obtained from the study shows that changing the stacking sequence and increasing the number of layers would improve the fatigue strength of the aluminum tube up to 40% for $[\pm 45]_{3s}$.

Chih-Yung Chang, *et al*, [9] studied the vibration behaviors of rotating composite shafts containing randomly oriented reinforcements. In order to account the interaction of finite concentrations of the reinforcements in the composite material they adopted the Mori-Tanaka mean-field theory. In their study, they expressed the effective elastic moduli of the composite material as a function of the phase properties, volume fraction, and orientation angles of its constituents. They also analyzed the dynamic responses of the laminated reinforced composite rotating shaft using four special cases of fiber inclusions. They performed this all by extending the finite element model of the rotating continuous fiber reinforced composite shafts derived previously by authors to the case that contains the fiber inclusions by taking these effective elastic moduli into account. Based on this model, they investigated the natural frequencies of the stationary shafts and the whirling speeds as well as the critical speeds of the rotating shafts. They also clearly demonstrated the importance of the orientations, aspect ratio and volume fraction of the fiber inclusions on the frequencies as well as the critical speeds of the composite shafts. Finally, they revealed from the result that the content and the orientation of the reinforcements have a great influence on the dynamics characteristics of the composite shafts.

K. G. Bang and D. G. Lee, [10] investigated the dynamic and static characteristics of carbon composite high speed air spindle through finite element analysis. They determined the thickness of the carbon composite shaft considering the bending natural frequency. They reinforced it circumferentially to enhance the radial stiffness of the air spindle. The bending

stiffness of the carbon composite shaft was also significantly improved by enhancement between the inner and middle parts of the shaft. The static stiffness of the air bearing was also substantially improved by enhancing the inner part of the shaft using the 90^0 plies. From results of the analysis they obtained, they determined that the stacking sequence to be $\left[(90)_2/(\pm 5)_4/(90)_2/(\pm 5)_4\right]_T$ considering the bending stiffness of the carbon composite shaft and the static stiffness of the air bearing. Finally, they evaluated the safety of the designed carbon composite shaft by considering residual thermal stresses, bending load and centrifugal force.

S. A. Mutasher [11] investigated the maximum torsional capacity of hybrid aluminum/composite shaft for different winding angle, number of layers and stacking sequences. The hybrid shaft he used consists of aluminum tube wound outside by E-glass and carbon fiber/epoxy composite. Finite element method has been used to analyze the hybrid shaft under static torsion. ANSYS finite element software was also used to perform the numerical analysis. He used to analyze the hybrid shaft using elasto-plastic properties for aluminum tube and linear elastic for composite materials. He also conducted experiments on the hybrid shaft by manufacturing a specimen the same as the model used in the ANSYS finite element software. Then he obtained good agreement between the finite element prediction and the experimental results. Both of the results showed that the static torque capacity was significantly affected by changing the winding angle, stacking sequences and number of layers. The maximum static torsion capacity of aluminum tube wound outside by six layers of carbon fiber/epoxy composite at winding angle of 45^0 was 295 Nm. Finally, the result from this combination gave him hybrid shaft that has high torque transmission capacity, higher fundamental natural bending frequency and less noise and vibration.

G.A. Riveros, [14] has studied the numerical evaluation of stress intensity factor, K_I using J-integral approach. He used Costal and Hydraulic Engineering Technical Note, CHETN to describe the numerical evaluation of the stress intensity factors using the J-integral approach. He calculated the stress intensity for semi-infinite plate with an edge crack. He obtained only a

difference of 1.25 percent between the closed-form and numerical solution. The CHEIN also helped him to perform detailed three-dimensional meshing of any complicated geometry. The meshing approach was used to generate a 3-D mesh of a hydraulic steel structure with multiple cracks. He also discussed the stress intensity factor for the 3-D problem with multiple cracks.

J. Dennis, *et al*, [15] made a research on shaft crack monitoring via torsional vibration analysis. Torsional vibration signature has shown them the potential to detect shaft cracks during normal machinery operations of rotating equipment. The method they used tracks characteristic changes in the natural torsional vibration frequencies that are associated with shaft crack propagation. The method is generally applicable to many types of rotating equipment. A laboratory scale rotor test bed was developed to investigate shaft cracking detection techniques under controlled conditions. They took a sample shaft with a semi-elliptical surface crack, which was propagated in three point bending. The fatigue crack was incrementally grown in nine steps, with depths ranging from approximately 0 – 60% of the shaft diameter. After the crack was grown to each pre-defined depth, the shaft was installed in the rotor test bed and the changes in shaft torsional vibration features observed. The first torsional natural frequency was shown to be sensitive to the shaft crack depth, which for the crack depths tested produced a 2 Hz frequency drop. The relationship between crack depth and torsional natural frequency is nonlinear. The test data show that changes in the torsional shaft frequency in the range of 0.1 to 0.2 Hz. can be detected by a visual inspection. This study points to the potential of using online torsional signature analysis as a diagnostic for shaft crack monitoring in rotating equipment.

P. R. Baviskar and V. B. Tungikar [26] studied on analysis of crack in shaft of blower using finite element analysis and experimental techniques. They came up with addressing inverse method for fault detection in moving parts. They suspected and concluded that one of the failures might be due to the crack initiation and propagation in any of moving parts. They also found that the natural frequency is monitored to access crack location and crack size in the beam because it is susceptible to minute changes. In their theoretical analysis, the crack was simulated by a spring connecting the two segments of the beam. They modeled the beam using

finite element method of analysis. The modal analysis of the beam was conducted using the ANSYS software whereas the experimentation was done on Fast Fourier Transformer Analyzer. The results they obtained from ANSYS and experimentation have good agreement.

3.2. Motivation

The literature survey highlighted that most of the analytical solutions are for drive shafts and rear axle of automobile and beams. Most of the researchers of the aforementioned literatures focus on the vibration analysis of beams. In addition, there are only few literatures which use fiber-reinforced composite materials alone for manufacturing of the drive shaft or rear axle. It is also known, that it is very difficult to find analytical solutions for complicated shapes like surfaces cracks on fiber-reinforced composite material shafts. So, most of the reviewed literatures use only finite element method as an alternative solution to get good results for variety of cracks, holes and ranges of loadings. Even the application of the concept for fracture mechanics approach to anisotropic material structures is very limited in view of the complexity of the deformation process.

Many of the works done by various researchers reveal that there are some finite element and few analytical solutions available for shafts and beams with holes and rarely available for surface cracks on fiber-reinforced composite material shafts. Most of these solutions deal with regular shape of cracks. The strength of the fiber-reinforced composite material is influenced by number of factors. These factors include anisotropic and non-homogeneous nature of the material, mechanical incompatibility of the constituent phases, the elastic and plastic behavior of the matrices and reinforcing materials, the volume fraction of the components, the direction of applied load and so on. Due to all these factors it is expected to have crack in or on surface of the shaft. The manufacturing process or assembly can also further induce flaws or cracks in the shaft.

Hence, these researches motivate concerned individuals to analyze the torque capacity, torsion buckling capacity and crack propagation of a transmission shaft combining using finite element

software ANSYS and analytical methods. It also motivates individuals to perform an experiment on the torque capacity of the shaft and finally to compare the results with those obtained from ANSYS and analytical calculations. It is also important to do this research because Dejen Aviation Engineering Complex needs to change the material of transmission shaft of Hidasie helicopter from carbon steel 6061 to fiber-reinforced composite material.

.

4. Design Analysis of transmission shaft

The glass fiber-reinforced composite hollow transmission shaft of the helicopter is going to be designed for torque capacity, buckling, and crack propagation. Therefore, it is important to know the current working condition of the transmission shaft.

4.1. Working condition of the transmission shaft

The transmission shaft of the helicopter is manufactured from a carbon steel 6061. It is plated on its outside with magnaflax in order to resist high temperature [20]. This transmission shaft transmits power from the main gear-box to intermediate gear-box. It is supported with a number of bearings at different distance which reduce the vibration on the transmission shaft. It is connected to both gear-boxes by spline mechanism at its ends. There is a male spline on both ends of the transmission shaft and a female spline on the gear-boxes.

The transmission shaft of the helicopter is outside of the fuselage which runs over tail fuselage as shown in figure 4-1. The bearings are inside the bearing holders which are fixed to the beam which runs from the main body of the helicopter to its tail rotor.

Figure 4-1: - H260L model helicopter

The mechanical and physical property of carbon steel 6061, the material used for the transmission shaft of H260L helicopter, is tabulated in table 4-1.

Table 4-1: - Mechanical and physical properties of carbon steel 6061 [20]

Mechanical/physical property	Quantity
Density	7860 kg/m^3
Yielding strength	250MPa
Ultimate strength	460MPa
Elastic modulus	210GPa
Shear modulus	80GPa
Poisson's ratio	0.3
Running speed of the shaft	3200-3400rpm
Diameter of the shaft	20mm
Length of the shaft	4m

The maximum recommended twisting angle of the transmission shaft of the helicopter is assumed to be 0.2 rad [20]. So it is possible to obtain the maximum torque transmitted by the transmission shaft to the intermediate gear-box using the numerical formula given below.

$$T = G\frac{\pi d^2}{32L}\varphi \text{.....(4.1)}$$

The torque obtained by substituting all the given data to the above numerical formula is $70\,Nm$. It is also possible to calculate the mass of the transmission shaft since we know the dimension and material type.

$$m = \rho V = \frac{\rho L \pi d^2}{4} \text{.....(4.2)}$$

Therefore, the transmission shaft has a mass of $10Kg$. This mass has to be reduced at the same time the strength and stiffness of the transmission shaft would increase as the fiber-reinforced composite material is used.

4.2. Manufacturing of the transmission shaft

The composite transmission shaft is designed to exploit an improvement in mechanical properties. The composite transmission shaft produced essentially for its physical and mechanical properties can play an important role during manufacturing. The strengths of fibers are generally much higher than those of their monolithic counterparts. There are of course many properties other than strength that we have to take into account when selecting reinforcement. In the case of fiber, the flexibility is important as it determines whether the fiber may be easily woven or not. This influences the choice of method for composite transmission shaft manufacturing. The flexibility of fiber depends on Young's modulus and diameter of the fiber. The flexibility of fiber decreases as diameter increases.

Clearly, because of their small cross-section dimensions, single fibers are not directly usable in composite transmission shaft applications. This problem may be overcome by embedding in a material that the fibers hold together, protect their surface from contact, and facilitate the production of composite transmission shaft. The embedding material is the matrix or resin.

The fiber and resin used for manufacturing of the composite transmission shaft are glass fiber and polyester respectively. A one cubic centimeter of catalyst is also added for every liter of polyester resin as hardener in order to facilitate the mixing process and drying.

The amount of reinforcement that can be incorporated in a given matrix is limited by a number of factors. For example with particulate-reinforced metals the reinforcement content is usually kept to less than 40% (0.4 volume fraction) owing to processing difficulties and increasing brittleness at higher contents. On the other hand, the processing methods for fiber-reinforced polymers are capable of producing composites with a high proportion of fibers, and the upper limit of about 70% (0.7 volume fractions) is set by the need to avoid fiber–fiber contact, which results in fiber damage [18]. The volume fraction of the glass fiber to polyester of the composite transmission shaft used for the experiment is 65%.

The manufacturing method used for the composite transmission shaft is filament winding method. There are two types of filament winding methods. These methods are biaxial and helical filament winding which are usually performed on automated machine. The specimens used for experimental testing are manufactured manually using the two filament winding methods together.

The winding machine consists of a turning device for the rotating mandrel, filament guide, resin impregnating bath and bobbin for roving as shown in figure 4-2. The transmission shaft is manufactured by setting different orientation angle on the mandrel by filament winding manually in winding shop of Dejen Aviation Engineering Complex, DAEC. Specimens of different orientation angle and stacking sequence were manufactured in order to decide which orientation angle and stacking sequence is better for the transmission shaft.

Figure 4-2: - Manufacturing of the hollow transmission shaft

Finally, due to the fact that the reinforcement is bounded by the matrix, any loads applied to the composite transmission shaft would be carried by both constituents. As in most cases, the reinforcement is the stiffer and stronger constituent than the matrix. It can be also taken as the principal load-bearer but the matrix main duty is to transfer the load to the reinforcement. The

composite transmission shaft produced by winding method is a multidirectional laminate which has strength in several directions.

The polyester resin used for the composite hollow transmission shaft manufacturing has its own physical and mechanical properties. These properties are tabulated in table 4-2. [21].

Table 4-2: - Some typical properties of polyester resin [18]

Property	Quantity
Density, ρ_m	1100-1250 kg/m^3
Service temperature, T	50-160 ^{0}C
Tensile strength, σ	50-70 MPa
Young's modulus, E_m	1300-4500 MPa
Thermal expansion, $\alpha_{th} in 10^{-6} K^{-1}$	100-200
Shear modulus, G_m^*	590Mpa
Poison's ratio, v_{12m}	0.28
Fracture toughness, K_{IC}, G_{IC}	$0.5\, MPa\sqrt{m}$

$$G^* = 0.5E(1+v)^{-1}$$

The choice of suitable reinforcing fiber should attach importance not only to the high strength but also to a low material density. Properties based on the material density are called specific material properties. One of these characteristics is usually taken as a measure not only the materials mechanical properties but also its low mass. So the reinforcing fiber used for the transmission shaft is glass fiber. Its specification is shown in table 4-3 [21].

Table 4-3: - Typical property of glass fiber [18]

property	quantity
Density, ρ_f	2540kg/m^3
Tensile strength, σ	2200Mpa
Modulus of elasticity, E_f	70Gpa
Poisson's ratio, v_{12f}	0.18
Shear modulus, G_f^*	30.9Gpa
Coefficient of thermal expansion	5x10^{-6} K^{-1}

$$G^* = 0.5E(1+v)^{-1}$$

The fabrication and properties of composites are strongly influenced by the proportions and properties of the matrix and the reinforcement. The proportions can be expressed either via the weight fraction, w which is relevant to fabrication, or via the volume fraction, v which is commonly used in property calculations. The definitions of w and v are related simply to the ratios of weight or volume.

When volume of fiber V_f and volume of matrix V_m are given in the volume of the composite V_c , the volume fraction of the fiber v_f and matrix v_m can be obtained [21] respectively as:

$$v_f = \frac{V_f}{V_c} \text{ and } v_m = \frac{V_m}{V_c} \quad \text{.....(4.3)}$$

The relation between the two volume fractions can be written as:

$$v_f + v_m = 1 \text{.....,,.....} \quad \text{(4.4)}$$

The weight fraction of fiber w_f and matrix w_m are obtained from the ratio of the weight of the fiber W_f to weight of the composite W_c and weight of the matrix W_m to the weight of the composite respectively. It is easy to find the weight fraction than volume fraction [21].

$$w_f = \frac{W_f}{W_c} \text{ and } w_m = \frac{W_m}{W_c} \quad \text{.....(4.5)}$$

The relation between the two weight fractions can be written as:

$$w_f + w_m = 1 \text{.....} \quad (4.6)$$

The density, ρ of the glass fiber-reinforced polyester polymer composite hollow transmission shaft can be obtained by using the volume fraction of the glass fiber and polyester matrix used for manufacturing.

$$\rho = v_f \rho_f + (1 - v_f)\rho_m \text{.....} \quad (4.7)$$

Using the above formula the density of the glass fiber-reinforced polyester composite material is obtained to be $2075 kg/m^3$.

It is necessary to determine the engineering constant for a plies in the shaft specimen laminate. These constants are modulus of elasticity of the ply along and transverse the fiber E_1 and E_2 respectively, shear modulus, G_{12} and Poisson's ratio, v_{12}. Thus, the elastic constants of the glass fiber-reinforced polyester polymer composite transmission shaft are calculated using Classic Laminate Theory, CLT based on the volume fraction of the fiber, v_f and the matrix as follows [21]:

$$E_1 = v_f E_f + (1 - v_f)E_m \text{.....} \quad (4.8)$$

$$E_2 = \frac{E_m^*(1 + 0.85 v_f^2)}{v_f \dfrac{E_m^*}{E_f} + (1 - v_f)^{1.25}} \quad \textit{where} \quad E_m^* = \frac{E_m}{1 - v_m^2} \text{.....} \quad (4.9)$$

$$G_{12} = \frac{G_m(1 + 0.6 v_f^{0.5})}{v_f \dfrac{G_m}{G_f} + (1 - v_f)^{1.25}} \text{.....} \quad (4.10)$$

$$v_{12} = v_f v_{12f} + (1 - v_f)v_{12m} \text{.....} \quad (4.11)$$

The glass fiber-reinforced polyester polymer composite transmission shaft from the resin and fiber using filament winding method has local coordinate system. This coordinate system is set

by using the fiber direction in winding, and the other two axes were produced by pointing perpendicular to that direction as shown in figure 4-3.

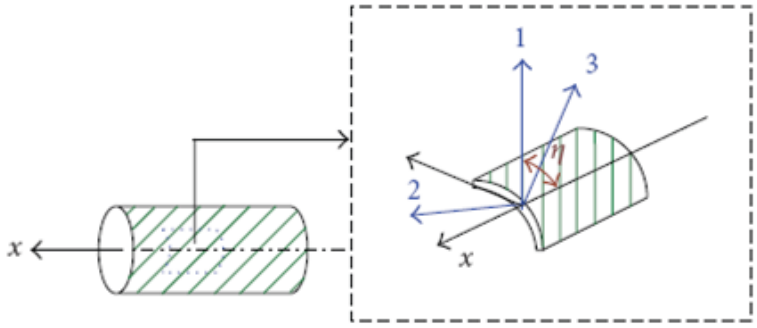

Figure 4-3: - The local and global coordinate of the transmission shaft

Therefore, from equations (4.8), (4.9), (4.10) and (4.11) the engineering constant of the glass fiber-reinforced polyester polymer composite transmission shaft is tabulated in table 4-4.

Table 4-4: - Engineering constants of the composite transmission shaft

Engineering constant	Result obtained
Longitudinal Modulus of Elasticity, E_1	$49\,Gpa$
Transverse Modulus of Elasticity, E_2	$21\,Gpa$
Shear Modulus of Elasticity, G_{12}	$3\,Gpa$
Poison's ratio, υ_{12}	0.215

The composite transmission shaft has an orthotropic plies. The plies rigidity $[Q]_{Esks}$ for the orthotropic plies in the ply coordinate system is as follows [21]:

$$[Q]_{Esks} = \begin{bmatrix} Q_{11} & Q_{12} & 0 \\ Q_{21} & Q_{22} & 0 \\ 0 & 0 & Q_{33} \end{bmatrix} \quad \text{.....(4.12)}$$

$$Q_{11} = Q_{22} = \frac{E_1}{1 - v_{12}^2 \frac{E_2}{E_1}}, \quad Q_{12} = Q_{21} = \frac{v_{12} E_1}{1 - v_{12}^2 \frac{E_2}{E_1}} \text{ and } Q_{33} = G_{12} \text{.....(4.13)}$$

Since the composite hollow transmission shaft is manufactured using winding method, it has fiber orientation angle. In order to select suitable and strong material to resist the applied torque, the composite hollow shaft with different thickness, stacking sequence and orientation angle were tested.

For the selected orientation angle, stacking sequence and thickness, the above ply rigidities are transformed from the local ply coordinate system, $[Q]_{Esks}$ to the global coordinate system, $[Q]_{lamks}$ as follow:

$$[Q]_{lamks} = [T][Q]_{Esks}[T]^T \text{.....(4.14)}$$

$$[T] = \begin{bmatrix} \cos^2 & \sin^2 & 2\sin\cos \\ \sin^2 & \cos^2 & -2\sin\cos \\ -\sin\cos & \sin\cos & \cos^2 - \sin^2 \end{bmatrix} \quad [T]^T = \begin{bmatrix} \cos^2 & \sin^2 & -\sin\cos \\ \sin^2 & \cos^2 & \sin\cos \\ 2\sin\cos & -2\sin\cos & \cos^2 - \sin^2 \end{bmatrix} \text{.....(4.15)}$$

This indicates for different angle orientation there is different plies rigidity in the global coordinate. The angle is positive when the local axis of the ply rotates in anticlockwise direction. The transformed rigidities of all plies weighted according to their cross sectional ratios are added together to yield a homogeneous laminate rigidity. The resulting laminate rigidity matrix $[A]$is:

$$[A] = \sum_{k=1}^{n} \frac{t_k}{t_{lam}} [Q]_{lamks} \text{.....(4.16)}$$

Where t_k, is thickness of a single ply and t_{lam}, is thickness of a laminate

Invert to obtain the laminate compliance matrix, $[a]$ as follow [21]:

$$[a] = [A]^{-1} \text{.....(4.17)}$$

The engineering constants for laminate in the global coordinate of the glass fiber-reinforced polyester polymer composite transmission shaft are obtained from the elements of compliance matrix.

$$E_{x,lam} = \frac{1}{a_{11}},\ E_{y,lam} = \frac{1}{a_{22}},\ G_{xy,lam} = G_{yx,lam} = \frac{1}{a_{33}},\ v_{xy,lam} = \frac{a_{21}}{a_{11}},\ v_{yx,lam} = \frac{a_{12}}{a_{22}} \quad \text{.....(4.18)}$$

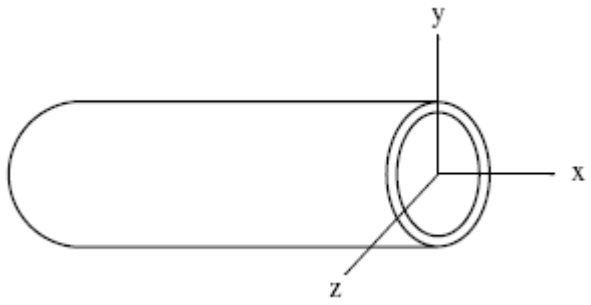

Figure 4-4: - Global coordinate of the transmission shaft

The engineering constant along the global coordinate for the fiber-reinforced composite transmission shaft manufactured from glass fiber and polyester resin are obtained based on equation (4.18) and tabulated in table 4-5. The engineering constants of the composite shaft for different orientation angle can be obtained base on a MATLAB code written in Appendix-A.

Table 4-5: - Engineering constants along the global coordinate

Engineering constant	Result
Young's Modulus in x-direction, $E_{x,lam}$	$38.6 Gpa$
Young's Modulus in y-direction, $E_{y,lam}$	$16.3 Gpa$
Shear Modulus in y-direction, $G_{xy,lam}$	$4.58 Gpa$
Shear Modulus in x-direction, $G_{yx,lam}$	$4.58 Gpa$
Poison's ratio y-direction, $v_{xy,lam}$	0.32
Poison's ratio x-direction, $v_{yx,lam}$	0.32

Therefore, the mechanical property for the hollow transmission shaft is as shown in table 4-6.

Table 4-6: - The mechanical properties for the glass fiber-reinforced composite [21]

Mechanical and physical property	Values
Density [Kg/m^3]	2075
Longitudinal Young's modulus, E_{xx} [GPa]	38.6
Transverse Young's modulus, E_{yy} [GPa]	16.3
Shear modulus, G_{xy} [GPa]	4.58
Poisson's ratio, υ	0.32
Glass fiber volume fraction, v_f of the composite	0.65
Longitudinal strength [MPa]	620
Transverse strength [MPa]	280

4.3. Design of torque capacity of transmission shaft

The helicopter has an engine which provides a power of 260HP. This power has to be transmitted to the main and tail rotor in order for the helicopter to fly on space. The power is transmitted from the engine to the tail rotor through main gear-box, transmission shaft, intermediate gear-box, tail transmission shaft, tail gear-box and finally to tail rotor. So the power, P which is transmitted to the transmission shaft, is calculated as follow [23]:

$$P = T\omega \quad \text{.....(4.19)}$$

Where T is the torque applied to the transmission shaft and ω is angular velocity [rad/sec] of the transmission shaft.

It is also possible to find the torque applied on transmission shaft if the frequency, f is known because the angular velocity can be obtained using the following formula [23].

$$\omega = 2\pi f \quad \text{.....(4.20)}$$

The torque that is applied on the transmission shaft can then be obtained if the frequency is known by substituting equation (4.20) into equation (4.19) and rearranging to give the following expression.

$$T = \frac{P}{2\pi f} \quad \text{.....(4.21)}$$

The angle of twisting per unit length, ϕ of the transmission shaft can be determined from the torque and the polar moment of inertia, J of the hollow transmission shaft.

$$\phi = \frac{T}{GJ} \quad \text{.....(4.22)}$$

The polar moment of inertia for hollow circular cross-section of a shaft is calculated as follows:

$$J = \frac{\pi\left(d_0^4 - d_i^4\right)}{32} \quad \text{.....(4.23)}$$

The dimensions of the shaft are dictated by the mode of failure, strength of the material associated with mode of failure, the required factor of safety and the shaft cross-section.

The shear stress, τ produced on the shaft due to the torque varies as the distance from the center of the shaft varies along the radial direction. Maximum shear stress is produced on the peripheral of the hollow transmission shaft. It can be obtained as follows [23]:

$$\tau = \frac{Tr}{J} \quad \text{.....(4.24)}$$

The helicopter engine speed is 3200rpm at power of 260HP [20]. The power is transferred to the transmission shaft which makes the transmission shaft to rotate at maximum speed of 1050rpm and minimum speed of 780rpm [20]. Therefore, the angular speed of the transmission shaft and the power transmitted by the transmission shaft can be calculated as:

$$\omega = \frac{3200 * 2\pi}{60} = 335 rad/\sec \quad and \quad P = 260 * 0.746 = 194 KW$$

Then the torque applied on the transmission shaft from equation (4.19) is obtained to be $580 Nm$.

So for allowable twisting angle, length of the transmission shaft, and diameter of the mandrel which is equal to the inside diameter of the transmission shaft, $d_i = 0.015m$, the outer diameter of the transmission shaft is obtained as follows by taking shear modulus to be $G = 4.58 GPa$ as shown in table 4-6.

$$d_0 = \sqrt[4]{d_i^4 + \frac{32TL^2}{\pi G\varphi}} = 35mm$$

The maximum shear stress produced on the transmission shaft due to the applied torque is on the peripheral of the shaft and is calculated by combining equations (4.23) and (4.24) as follows:

$$\tau_{\max} = \frac{16Td_0}{\pi\left(d_0^4 - d_i^4\right)} = 75MPa$$

It is possible also to determine the frequency of the transmission shaft from equation (4.20) as follows:

$$f = \frac{\omega}{2\pi} = 53Hz$$

Therefore, the mass of the glass fiber-reinforced polyester polymer composite hollow transmission shaft can be calculated since its density and dimension are determined. The mass is then equal to:

$$m = \rho V = \frac{\rho L\pi\left(d_0^2 - d_i^2\right)}{4} = 6.5kg$$

In the cylindrical coordinate (r,θ,z) the displacement field of the transmission hollow shaft under torsion is obtained by assuming $u = 0$, $v = (r,z)$ and $w = 0$. On the basis of linear theory of elasticity, only shear strain components $\gamma_{r\theta}$ and $\gamma_{z\theta}$ exist. Hence, the only nonzero shear stress components, according to Hook's law, are as follows [24, 25]:

$$\tau_{r\theta} = G\gamma_{r\theta} = G\left(\frac{\partial v}{\partial r} - \frac{v}{r}\right) \text{.....(4.25)}$$

$$\tau_{z\theta} = G\gamma_{z\theta} = G\frac{\partial v}{\partial z} \text{.....(4.26)}$$

The stress field in equations (4.25) and (4.26) allows traction in circumferential direction that is related to the distributed twisting moment or torque but not in radial and longitudinal directions on the lateral surfaces. The only equilibrium equation [25] to be satisfied for this stress filed of the transmission shaft is the following:

$$\frac{\partial}{\partial r}\left(r^2\tau_{r\theta}\right)+\frac{\partial}{\partial z}\left(r^2\tau_{z\theta}\right)=0 \quad \text{.....(4.27)}$$

Substituting equations (4.25) and (4.26) into equation (4.27), one obtains the equilibrium equation governing the circumferential displacement, v as follows:

$$\frac{\partial}{\partial r}\left[r^3\frac{\partial}{\partial r}\left(\frac{v}{r}\right)\right]+r^2\frac{\partial^2 v}{\partial z^2}=0 \quad \text{.....(4.28)}$$

The boundary conditions along the lateral surface of the transmission shaft at $r=r_i$ and r_0 are $\tau_{r\theta}=\tau_{\min}$ and $\tau_{\max}$, respectively; where r_i is the inner radius of the shaft, and r_0 is the radius of the outer surface.

Assuming uniform $\tau_{r\theta}$ along the circumferential direction, the magnitudes of applied distributed torques are $T_{r_i}=2\pi r_i^2\tau_{\min}$ and $T_{r_0}=2\pi r_0^2\tau_{\max}$ at $r=r_i$ and $r=r_0$, respectively. The twisting moment T at each section is related to the shearing stress $\tau_{z\theta}$ as follows [25]:

$$T=2\pi\int_{r_i}^{r_0}\tau_{z\theta}r^2dr=2\pi G\int_{r_i}^{r_0}\frac{\partial v}{\partial z}r^2dr \quad \text{.....(4.29)}$$

For the technical theory of the circular transmission shaft under torsion, v and, subsequently, $\tau_{z\theta}$ are considered to vary as linear function of r.

4.4. Torsional buckling capacity

The transmission shaft of the helicopter has to be identified whether it is long shaft or short & medium shaft. Long or short and medium shafts have different way of analysis for their torsional buckling capacity. The following expression is used to determine whether a shaft is long or short and medium [28].

$$\frac{1}{\sqrt{1-\upsilon^2}}\frac{L^2t}{(2r)^3} \quad \text{.....(4.30)}$$

If the result of equation (4.30) is greater than 5.5, then the transmission shaft is long but if it is less than 5.5, it is short and medium transmission shaft. The result of equation (4.30) is then greater than 5.5. So the transmission shaft is long shaft.

The critical shear stress, τ_{cr} for long transmission shaft due to the torque applied on it is calculated using the following expression.

$$\tau_{cr} = \frac{E}{3\sqrt{2}(1-\upsilon^2)^{3/4}}(t/r)^{3/2} \quad \text{.....(4.31)}$$

The critical shear stress of the transmission shaft is $426\,MPa$ which is obtained from equation (4.31). There is also a relation between the torsional buckling capacity, T_{cr} and critical shear stress of the transmission shaft. The expression which relates the two quantities is given by:

$$T_{cr} = \tau_{cr} 2\pi r^2 t \quad \text{.....(4.32)}$$

The critical torsional buckling is obtained to be $8.2KNm$ from equation (4.32) which is greater than the actual load which the transmission shaft is loaded to.

Since long thin hollow transmission shafts are vulnerable to torsional buckling, the possibility of the torsional buckling of the composite shaft was checked by expression for the torsional buckling load, T_{cr} of a thin walled orthotropic tube, which is expressed as below [29].

$$T_{cr} = (2\pi^2 t)(0.272)(E_x E_y^3)^{0.5}(t/r)^{1.5} \quad \text{.....(4.33)}$$

This equation has been generated from the equation of isotropic cylindrical shell and has been used for the design of drive shafts [29]. From the above equation, it can be seen that the torsional buckling capacity of composite transmission shaft is strongly dependent on the thickness of composite shaft and the average modulus in hoop direction.

4.5. Crack propagation analysis

The composite transmission shaft is subjected to a torque from the intermediate gear-box of the helicopter. This indicates if the transmission shaft has any flaw it will experience the three type of loading modes of crack. These are Mode-I loading, where the principal load is applied normal to the crack plane tend to open the crack, Mode-II loading, corresponds to in-plane shear loading and tends to slide one crack face with respect to the other and Mode-III loading, refers to out-of-plane shear [32].

In the Mode-I, or opening mode, the body is loaded by tensile forces such that the crack surfaces are pulled apart in the y direction as shown in Figure 4-5. The deformations are then symmetric with respect to the planes perpendicular to the y axis and the z axis.

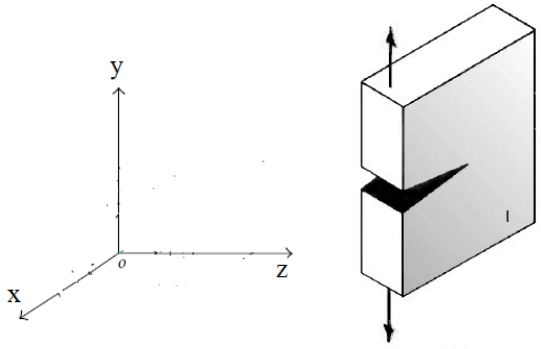

Figure 4-5: - Mode-I, opening mode of loading

In the Mode-II, or sliding mode, the body is loaded by shear forces parallel to the crack surfaces, which slide over each other in the x direction as shown in figure 4-6. The deformations are then symmetric with respect to the plane perpendicular to the z axis and skew symmetric with respect to the plane perpendicular to the y axis [32].

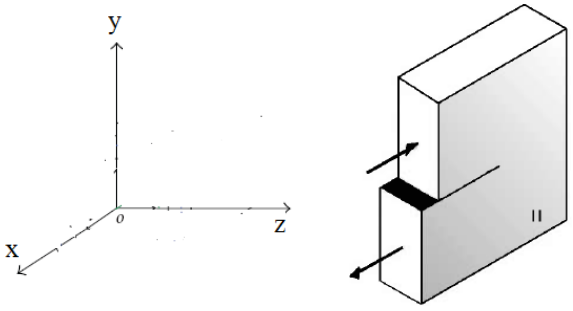

Figure 4-6: - Mode-II, sliding mode of loading

Finally, in the Mode-III, or tearing mode, the body is loaded by shear forces parallel to the crack front the crack surfaces and the crack surfaces slide over each other in the z direction as shown in figure 4-7. The deformations are then skew-symmetric with respect to the plane perpendicular to the z and the y axis [32].

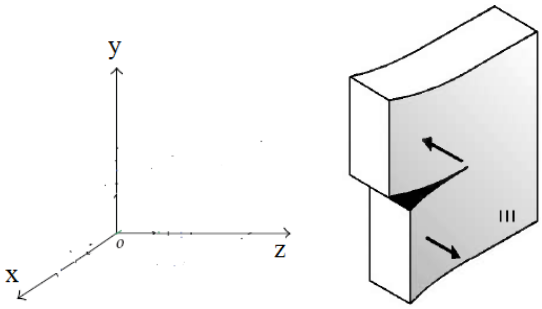

Figure 4-7: - Mode-III, tearing mode of loading

For each of the above modes, crack extension may take place only in the direction of the x axis as it is the original orientation (direction) of the crack. In a more general situation, we may typically find a mixed mode situation. For such cases a superposition of the modes is the best solution that has to be taken. In a linear elastic mixed mode situation, the principle of stress superposition states that the individual contributions to a given stress component are additive. So if σ_{ij}^{I}, σ_{ij}^{II} and σ_{ij}^{III} are the stress components associated to the modes-I, II and III respectively, then the stress component σ_{ij} is given by the following expression [33].

$$\sigma_{ij} = \sigma_{ij}^{I} + \sigma_{ij}^{II} + \sigma_{ij}^{III} \quad \text{.....(4.34)}$$
$$for\ i, j = x, y$$

The transmission shaft of the helicopter is subjected to torsion as it is described in section 4.3. It is considered to be torsional problem when the applied moment or torque twists the transmission shaft about its longitudinal axis as shown in figure 4-8. The maximum shear stress that can be developed due to the applied torque was obtained analytically in section 4.3.

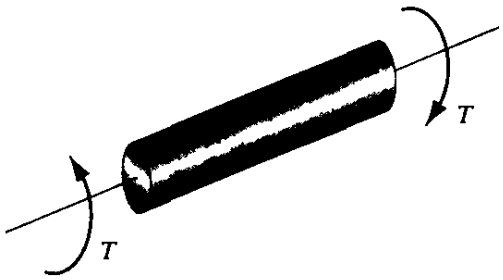

Figure 4-8: - Transmission shaft subjected to torque

We can take a small area from the transmission shaft where the maximum shear stress is obtained. In that small area we can take the shear stress as a remote tensile stress for a central crack through-thickness as shown in Figure 4-9. This remote tensile stress will have an opening mode of fracture on the central crack. Even though, they are not that much significant, it is obvious that there is also a sliding and tearing mode of fracture in the transmission shaft. But let's assume that we have only an opening mode of fracture.

It is assumed that the crack propagation is going to be analyzed using Linear Elastic Fracture Mechanics, LEFM. It is also assumed that the transmission shaft is subjected to plane strain in order to obtain the stress intensity factor, SIF.

For a through-thickness central crack size of $2a$, width of b and a remote tensile stress of σ as shown in figure 4-9, stress intensity factor, K_I can be obtained analytically using the following expression [27].

$$K_I = C\sigma\sqrt{\pi a} \quad \text{.....(4.35)}$$

$$\textit{Where} \quad C = (1 - 0.1\eta^2 + 0.96\eta^4)\sqrt{1/\cos(\pi\eta)}$$

$$\eta = \frac{a}{b}$$

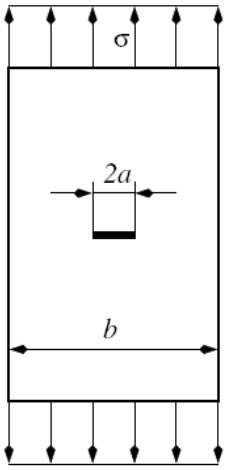

Figure 4-9: - Through-thickness central crack

Consider a finite glass fiber-reinforced polyester polymer composite plate with width, $b = 0.2m$ and half crack size, $a = 0.02m$ so the stress intensity factor, K_I of the opening mode of fracture is $19\,Mpa\sqrt{m}$.

Now consider any of the three modes we have introduced. Within the scope of the theory of linear elasticity, a crack introduces a discontinuity in the elastic body such that the stresses tend to infinity as one approach the crack tip. Using the semi-inverse method of Westerngaard, Irwin related the singular behavior of the stress components to the distance to the crack tip r. The relation he obtained can be written in a simplified form as [34]

$$\sigma \cong \frac{K_I}{\sqrt{2\pi r}} \qquad \text{.....(4.36)}$$

The parameter K, the stress intensity factor, plays a fundamental role in fracture mechanics, as it characterizes the stress field in this region. So the stress that will be developed near the crack tip due to the discontinuity can be approximated using equation (4.36) and tabulated in table 4-7 as a function of the distance r from the crack tip. As shown in table 4-7 the stress increases as the distance r decreases. This indicates there will be maximum stress just at the tip of the crack.

Table 4-7: - Stress near the crack tip of a through-thickness central crack

Distance, r from the crack tip in meter	Stress, σ in MPa
0.01	75
0.009	80
0.007	91
0.005	107
0.003	138
0.002	170
0.001	240
0.0009	253
0.0007	287

Henceforth, we will consider the problem of a cracked glass fiber-reinforced composite plate in a plane stress situation, which means that Mode-III situations will be disregarded. And then we consider only the two mode of fracture. This will help to analyze the general and the real world situation of the transmission shaft of the helicopter.

Let's consider a static crack in a glass fiber-reinforced polyester polymer composite plate which is in a plane stress situation in order to find the stress in general. Assume that the crack surfaces are free of stress and that the crack is positioned along the negative x-axis, as shown in the figure 4-10.

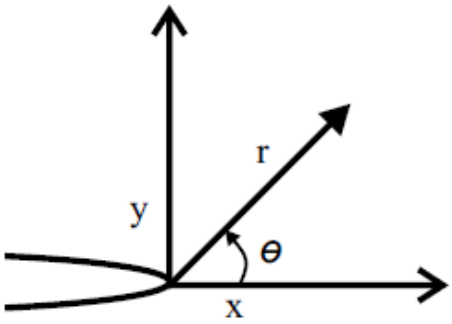

Figure 4-10: - Crack tip polar coordinate

Then the distribution of the stresses in the region near the tip of the crack may be derived as an interior asymptotic expansion [35]. In polar coordinates, we have the stresses near the tip of the crack as:

$$\sigma_{ij}(r,\theta) = \frac{K_I}{\sqrt{2\pi r}} f_{ij}^{I}(\theta) + \frac{K_{II}}{\sqrt{2\pi r}} f_{ij}^{II}(\theta) + \sigma_{ij}^{0} \quad \text{.....(4.37)}$$

The above equation is for $r \to 0$ and $i, j = x, y$ and σ_{ij}^{0} indicates the finite stresses at the crack tip. Here the normalizing constants for the symmetric and anti-symmetric parts of the stress field of K_I and K_{II} represent respectively the stress intensity factors for the corresponding modes I and II. These are defined by the following expressions [35].

$$K_I = \lim_{r\to 0} \sqrt{2\pi r}\,\sigma_{yy}(r,0) \quad \text{.....(4.38}a\text{)}$$

$$K_{II} = \lim_{r\to 0} \sqrt{2\pi r}\,\sigma_{xy}(r,0) \quad \text{.....(4.38}b\text{)}$$

The stress varies as the function of polar angle, θ indicted in Figure 4-10. The angular variation functions for Mode-I are given respectively by the following expression [35].

$$f_{xx}^{I}(\theta) = \cos\left(\frac{\theta}{2}\right)\left(1 - \sin\left(\frac{\theta}{2}\right)\sin\left(\frac{3\theta}{2}\right)\right) \quad \text{.....(4.39}a\text{)}$$

$$f_{yy}^{I}(\theta) = \cos\left(\frac{\theta}{2}\right)\left(1 + \sin\left(\frac{\theta}{2}\right)\sin\left(\frac{3\theta}{2}\right)\right) \quad \text{.....(4.39}b\text{)}$$

$$f_{xy}^{I}(\theta) = \cos\left(\frac{\theta}{2}\right)\sin\left(\frac{\theta}{2}\right)\sin\left(\frac{3\theta}{2}\right) \quad \text{.....(4.39}c\text{)}$$

While the equivalent functions for Mode-II are the followings.

$$f_{xx}^{II}(\theta) = -\sin\left(\frac{\theta}{2}\right)\left(2+\cos\left(\frac{\theta}{2}\right)\cos\left(\frac{3\theta}{2}\right)\right) \quad \text{.....(4.40}a\text{)}$$

$$f_{yy}^{II}(\theta) = \cos\left(\frac{\theta}{2}\right)\sin\left(\frac{\theta}{2}\right)\sin\left(\frac{3\theta}{2}\right) \quad \text{.....(4.40}b\text{)}$$

$$f_{xy}^{II}(\theta) = \cos\left(\frac{\theta}{2}\right)\left(1-\sin\left(\frac{\theta}{2}\right)\sin\left(\frac{3\theta}{2}\right)\right) \quad \text{.....(4.40}c\text{)}$$

It is also possible to find the corresponding displacement field near the crack tip of the glass fiber-reinforced polyester polymer composites plate, which is discontinuous over the crack. This displacement field is obtained using the following expression [35].

$$u_i(r,\theta) = u_i^0 + \frac{K_I}{G}\sqrt{\frac{r}{2\pi}}f_i^I(\theta) + \frac{K_{II}}{G}\sqrt{\frac{r}{2\pi}}f_i^{II}(\theta) \quad \text{.....(4.41)}$$

Where $i = x, y$ and for $r \to 0$ and here, u_i^0 are the crack tip displacements. The angular variation functions here are now given by

$$f_x^I(\theta) = \cos\left(\frac{\theta}{2}\right)\left(\frac{1-\upsilon}{1+\upsilon}+\sin^2\left(\frac{\theta}{2}\right)\right) \quad \text{.....(4.42}a\text{)}$$

$$f_y^I(\theta) = \sin\left(\frac{\theta}{2}\right)\left(\frac{2}{1+\upsilon}-\cos^2\left(\frac{\theta}{2}\right)\right) \quad \text{.....(4.42}b\text{)}$$

$$f_y^{II}(\theta) = \sin\left(\frac{\theta}{2}\right)\left(\frac{2}{1+\upsilon}+\cos^2\left(\frac{\theta}{2}\right)\right) \quad \text{.....(4.42}c\text{)}$$

$$f_x^{II}(\theta) = \cos\left(\frac{\theta}{2}\right)\left(-\frac{1-\upsilon}{1+\upsilon}+\sin^2\left(\frac{\theta}{2}\right)\right) \quad \text{.....(4.42}d\text{)}$$

The formulas we have presented allow us to have a characterization of the stresses and the displacements in the vicinity of a crack tip of the glass fiber-reinforced polyester polymer composite plate with through-thickness central crack.

.

5. Finite element analysis

5.1. Introduction

Finite element analysis, FEA is a computer-based numerical technique for calculating the strength and behavior of engineering structures. It can be used to calculate deflection, stress, vibration, buckling behavior and many other phenomena. It can also be used to analyze either small or large-scale deflection under loading or applied displacement [22]. It uses a numerical technique called the finite element method, FEM. In finite element method, the actual continuum is represented by the finite elements. These elements are considered to be joined at specified joints called nodes or nodal points [36]. As the actual variation of the field variable (like displacement, temperature and pressure or velocity) inside the continuum is not known, the variation of the field variable inside a finite element is approximated by a simple function. The approximating functions are also called interpolation models and are defined in terms of field variable at the nodes. When the equilibrium equations for the whole continuum are known, the unknowns will be the nodal values of the field variable [22].

In this research finite element analysis is carried out using the FEA software ANSYS. ANSYS is a general purpose finite element modeling package for numerically solving a wide variety of mechanical problems. These problems include both linear and nonlinear static and dynamic structural analysis, heat transfer, fluid mechanics problems as well as acoustic and electromagnetic problems [22].

The primary unknowns in this structural analysis are angular displacements and other quantities such as strains, torsional stresses, stress intensity factor, and reaction forces. These all are then derived from the nodal displacements.

ANSYS 12.0 Classic is used to develop the required 3-D finite element model of the transmission shaft. This section explains in detail the geometry and material property of

laminated composite material, step wise procedure to develop the composite finite element model, and the boundary and loading conditions applied on the model.

5.2. Modeling the composite shaft

A full length Finite Element, FE model is constructed for the 200 mm long hollow circular composite shaft under static torsion load. 3-D 8 nodes SOLID46 element was used to develop the required 3D composite shaft model. In the 3-D composite shaft model, each layer in the laminate is mapped meshed separately in thickness direction with different element coordinate system to represent a composite layer arrangement. This means, each layer on the hollow transmission shaft is modeled as a separate volume and meshed using SOLID46 elements. SOLID46 is a layered version of 8-node structure solid designed to model layered thick solids. This element allows up to 250 different material layers with different orientations and orthotropic material properties in each layer [36]. If more than 250 layers are required, a user-input constitutive matrix option is available. The element may also be stacked as an alternative approach. The element has three degrees of freedom, DOF at each node and translations in the nodal x, y, and z directions [36]. The layers were assumed perfectly bonded. The mapping mesh technique was used for the entire domain as shown in figure 5-1.

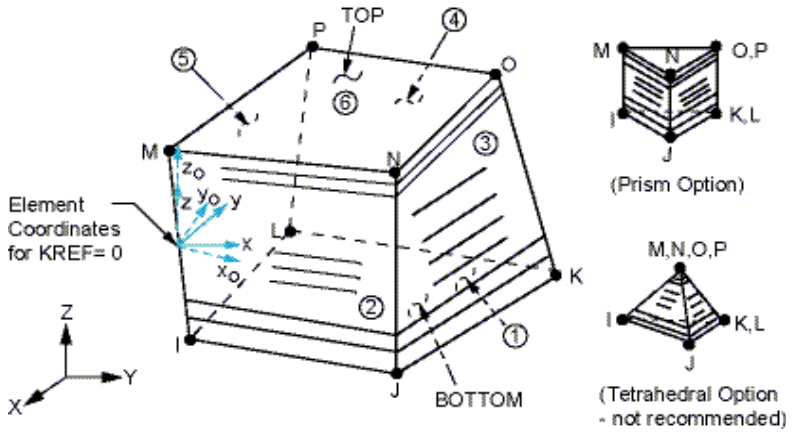

x_o = Element x-axis if ESYS is not supplied.

x = Element x-axis if ESYS is supplied.

Figure 5-1: - Solid46 DOF and element type

The following procedure was used to create the 3-D finite element model of the composite hollow transmission shaft and generate mesh.

1. 3D 8 nodes SOLID46 elements were defined as element type. Unidirectional orthotropic material properties for lamina were defined in material property section.
2. The hollow transmission shaft was modeled sequentially in step wise. First, the concentric circles which enclose the area then, 3D hollow shaft. Each laminate was modeled layer by layer.
3. The material property was given in preprocessor of material model for the modeled transmission shaft.
4. The boundary condition of the transmission shaft was given. The displacement constraint at one end and applied moment/force at the other of the transmission shaft
5. The volume was mapped meshed. After mapped meshing of the first layer volume, the 3-D element mesh generated in the XY plane at Z=0 can be seen.
6. In this model, 3 element coordinate system was created corresponding to each fiber orientation of each layer in the composite laminate. Then again, the coordinate system was reset to global coordinate system.
7. The second layer in the Sub-laminate was created by selecting the corresponding element coordinate system and SOLID46 element, and then extruding the top area of layer one.
8. Same procedure was followed to generate other layer in the laminate by choosing the corresponding element coordinate system. After extruding all layer of Sub-laminate, the meshing can be seen.
9. The lines representing the length were selected and number divisions for the mapped mesh was specified. The number of division and spacing ratio in the lines was given same as the numbers for the lines in the volume created for Sub-laminate. The other lines in the volume were selected and number of divisions for the mapped mesh was specified. This was to ensure proper sizing of elements for merging of nodes.
10. Finally, solve the modeled transmission shaft under the solution main menu and see the results on the postprocessor menu.

In general, phenomenological strength criteria such as maximum stress and Von Misses criteria are used to detect the failure status of the composite laminates. Due to the complexity of failure mechanisms in the hollow composite transmission shaft, it is difficult to define an applicable failure criterion. However, it is expected that shear failure of the hollow composite shaft is dominated by properties of glass fiber-reinforced polyester polymer composite layers, and the laminate fails just after the shear strain reached maximum failure strain from experimental results in any direction. So, the maximum strain failure criterion was used to predict the failure load in this study.

5.2.1. Material properties

The elastic engineering constants were found using Classic Laminate Theory, CLT for composite materials. The properties were used with conventional laminate theory to calculate the theoretical effective properties of the orthotropic monolithic model. The material used for the composite laminate is E-glass fiber-reinforced polyester polymer laminate. The glass fiber-reinforced polyester polymer layers were modeled with homogenized linear elastic orthotropic materials. The unidirectional layer orthotropic properties from equations (4.8) – (4.11) for the transmission shaft material are given as:

$$E_1 = 49\ GPa \quad E_2 = E_3 = 21 GPa$$
$$v_{12} = v_{23} = v_{13} = 0.215$$
$$G_{12} = G_{23} = G_{13} = 3GPa$$

Where E_1, E_2 and E_3 are the Young's moduli of the composite lamina along the material coordinates. G_{12}, G_{23} and G_{13} are the Shear moduli and v_{12}, v_{23} and v_{13} are Poisson's ratio with respect to the 1-2, 2-3 and 1-3 planes, respectively as shown in Figure 4-4 in section 4.2.

5.2.2. Boundary conditions

The aim is to model the transmission shaft in FEA subjected to pure torsion. So for this condition, one end of the transmission shaft is assumed fixed with all the DOF and the other end is subjected to applied torque which is a distributed forces in tangential direction to the

outside of the fixture of the hollow transmission shaft. The distributed forces can be calculated by converting the applied torque to the tangential force and multiplying by outside diameter and dividing the same by number of nodes on the side of the fixture of the transmission shaft model.

In order to restrict the movement of the nodes in the radial direction at the end at which the force is applied, the DOF in r-direction is protected. The nodes are to be rotated along cylindrical coordinate system so that the applied forces in nodal Θ-direction are tangential to the perimeter of the shaft. No cantilever effect will be formed since the forces will deform the shaft about its axis by pure twisting.

5.2.3. Input Data

The element is defined by eight nodes, layer thicknesses, layer material direction angles, and orthotropic material properties. Shear moduli G_{XZ} and G_{YZ} must be within a factor of 10,000 of each other.

The element z-axis is defined to be normal to a flat reference plane, using real constant KREF. KREF may have values of 0 (mid-plane), 1 (bottom), or 2 (top). If the nodes imply a warped surface, an averaged flat plane is used. The default element x-axis is the projection of side I-J, side M-N, or their average (depending on KREF) onto the reference plane. The orientation within the plane of the layers may be changed [36].

A triangular-shaped element may be formed by defining the same node number for nodes K, L and O. the input may be either in matrix form or layer form, depending upon KEYOPT (2). Briefly, the force-strain and moment-curvature relationships defining the matrices for a linear variation of strain through the thickness (KEYOPT (2) =2) may be defined as [36]:

$$\begin{Bmatrix} N \\ M \end{Bmatrix} = \begin{bmatrix} A & B \\ B & D \end{bmatrix} \begin{Bmatrix} E \\ K \end{Bmatrix} - \begin{Bmatrix} MT \\ BT \end{Bmatrix}$$

$$[A]=\begin{bmatrix} A_1 & A_2 & A_3 & A_4 & A_5 & A_6 \\ A_2 & A_7 & A_8 & A_9 & A_{10} & A_{11} \\ A_3 & A_8 & A_{12} & A_{13} & A_{14} & A_{15} \\ A_4 & A_9 & A_{13} & A_{16} & A_{17} & A_{18} \\ A_5 & A_{10} & A_{15} & A_{17} & A_{19} & A_{20} \\ A_6 & A_{11} & A_{16} & A_{18} & A_{20} & A_{21} \end{bmatrix} Or\ [A]=\begin{bmatrix} A_1 & A_2 & A_3 \\ A_2 & A_4 & A_5 \\ A_3 & A_5 & A_6 \end{bmatrix}$$

Sub matrices [B] and [D] are input similarly. Note that sub matrices are symmetric. {MT} and {BT} are for thermal effects. The layer number (LN) can range from 1 to 250. In this local right-handed system, the x'-axis is rotated an angle THETA (LN) (in degrees) from the element x-axis toward the element y-axis. The total number of layers must be specified (NL). The properties of all layers should be entered (LSYM=0) if the properties of the layers are symmetrical about the mid-thickness of the element (LSYM=1), only half of properties of the layers, up to and including the middle layer (if any), need to be entered. While all layers may be printed, two layers may be specifically selected to be output (LP1 and LP2, with LP1 usually less than LP2) [36].

5.3. Torque capacity analysis on ANSYS

Based on the above procedure, the composite hollow transmission shaft is modeled using ANSYS, which is used for pre and post-processing of the model with FEA as the solver. The model is created in the pre-processing stage of the model and the results are viewed in post-processing stage. As it has been explained, the composite hollow transmission shaft is created using linear layered SOLID46 element. The properties of the laminates are given as input using ANSYS material library. The composite transmission shaft is modeled with different angle orientation and stacking sequence. The suitable stacking sequence for the transmission shaft is shown in figure 5-2. This stacking sequence is modeled on ANSYS in order to analyze the transmission shaft for its torque capacity. The zoomed 3-D model of the transmission shaft on ANSYS is shown in figure 5-3.

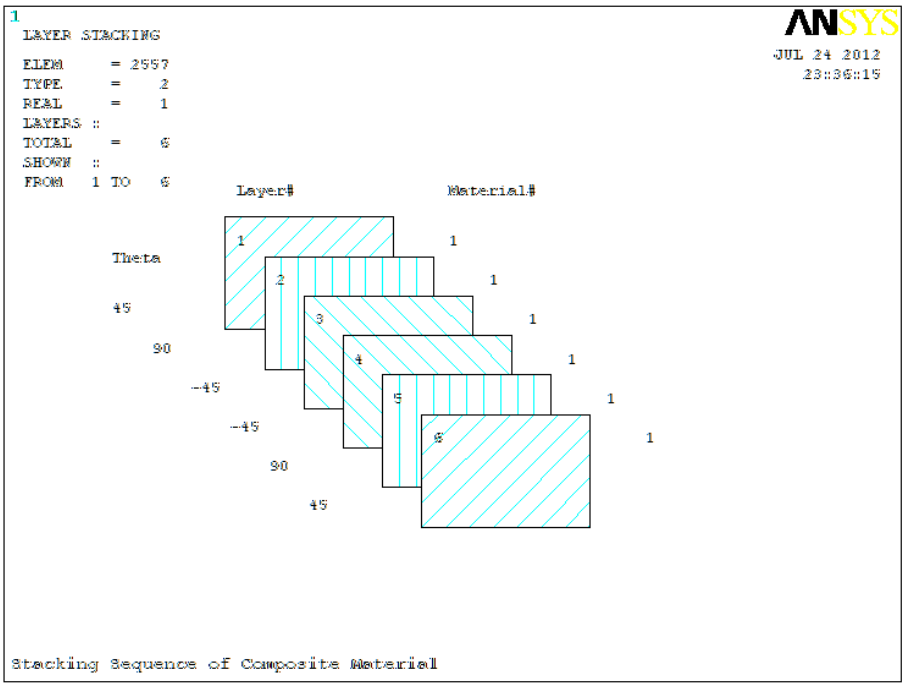

Figure 5-2: - The stacking sequence for the transmission shaft

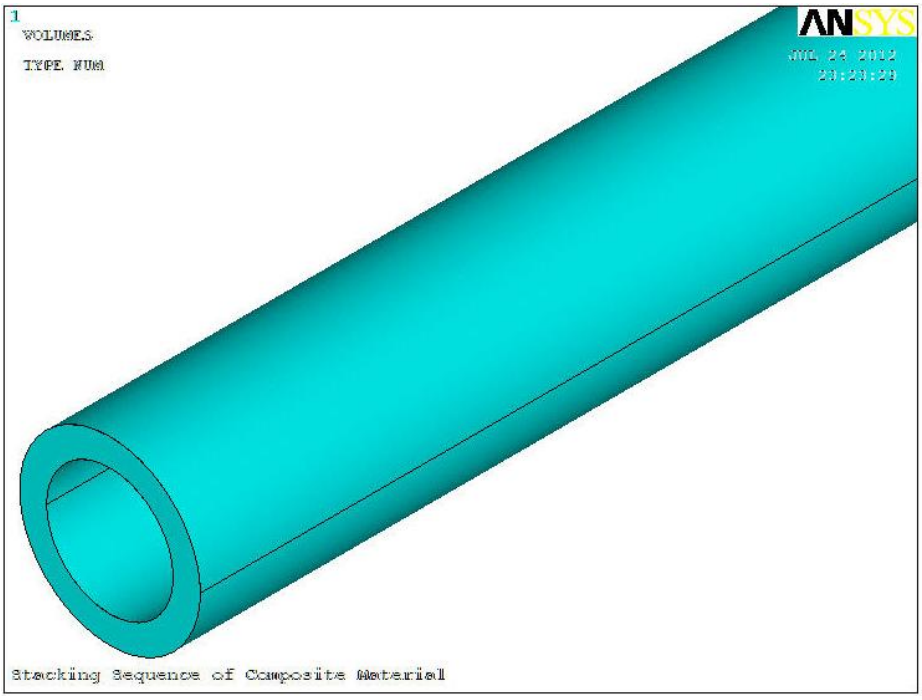

Figure 5-3: - The zoomed 3D model of the transmission shaft

When the transmission shaft is analyzed for torque capacity its model has to discrete into finite elements in order to get an accurate result for shear stress. In ANSYS to get the approximate results the model has to be meshed. The model is mapped meshed by specifying the line which represents the mesh, number of divisions and spacing ratio. The zoomed meshed model of the transmission shaft is shown in figure 5-4.

The stress on the transmission shaft is obtained by applying the boundary conditions. The boundary conditions for the transmission shaft are the applied torque and the DOF. The transmission shaft is assumed fixed in all DOF at one end and Subjected to torque at the other end. The torque of the transmission is given by converting into applied force at its peripheral using its outside diameter. The Von Misses stress obtained from ANSYS is shown in figure 5-5. The maximum stress is shown at the end of the shaft because it increases with its length.

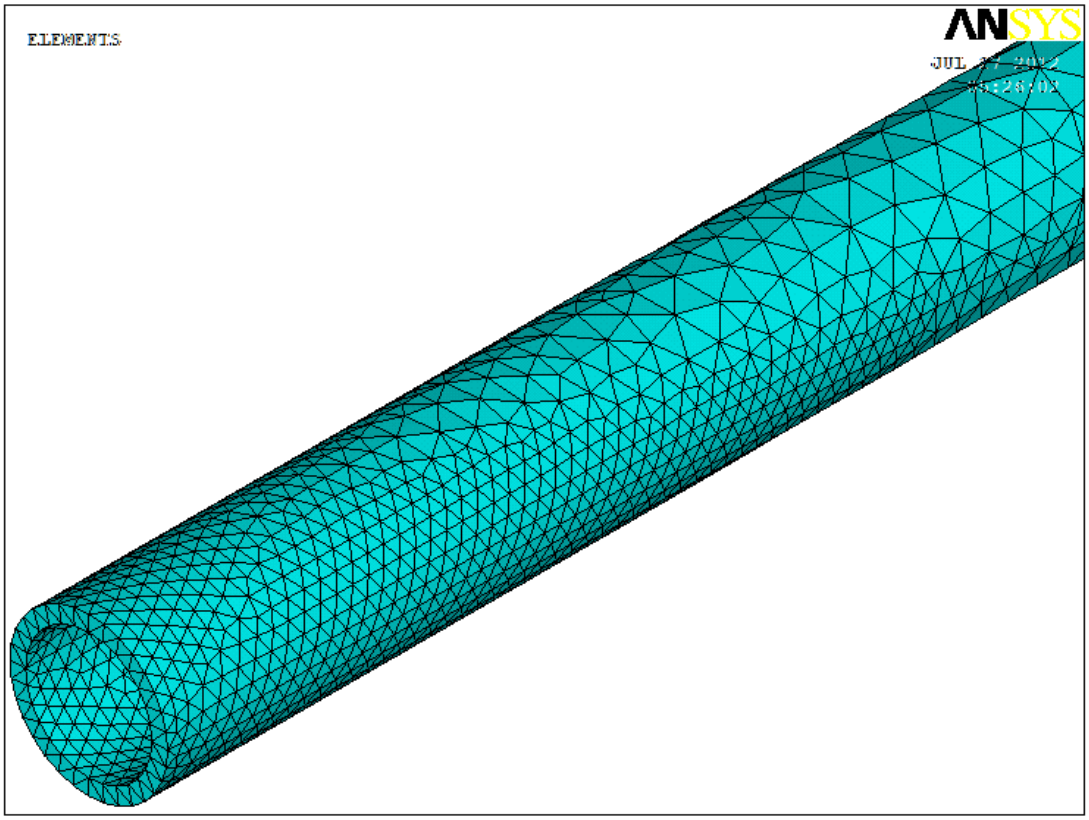

Figure 5-4: - Zoomed Meshed model of the transmission shaft

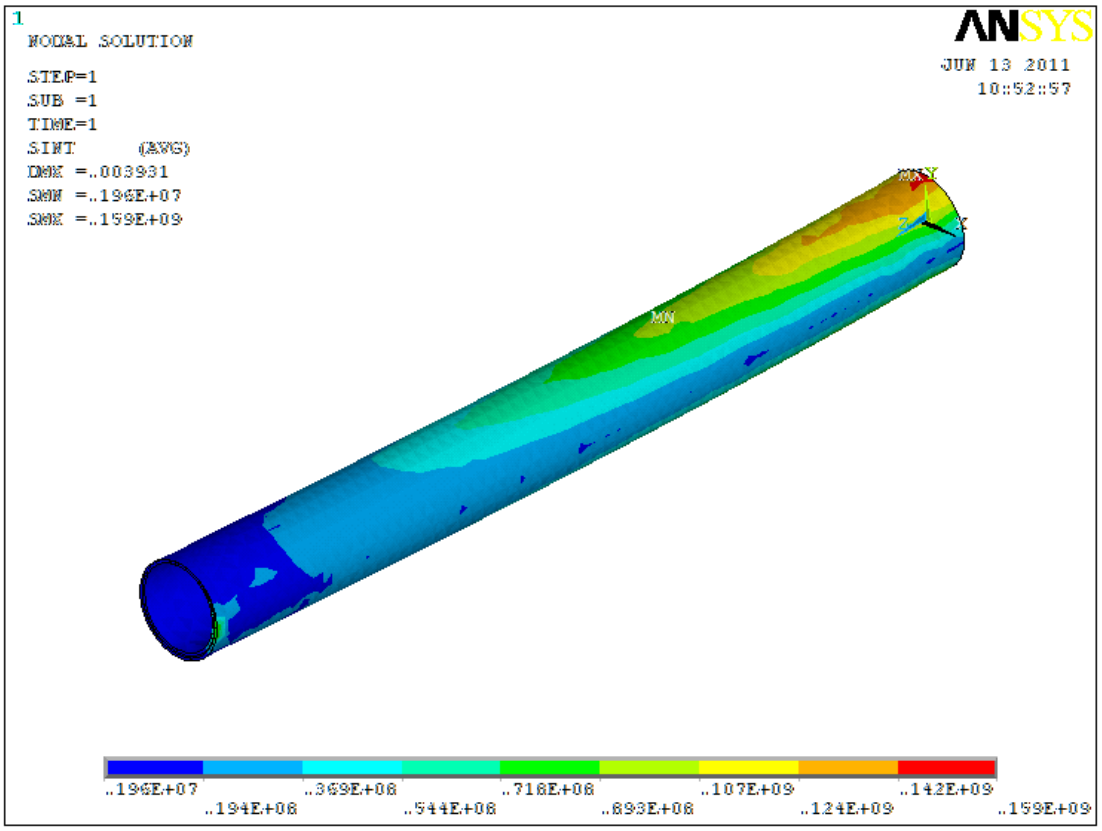

Figure 5-5: - Von Misses stress of the transmission shaft

5.4. Crack propagation analysis on ANSYS

The crack propagation of the transmission shaft on ANSYS can be analyzed by taking an infinitesimal part from it using LEFM. Since the transmission shaft is subjected to shear stress, we can assume an opening mode of fracture mechanics on a plate with through-thickness central crack. A sharp central crack is assumed since it is the worst in crack propagation. It develops large stress concentration at its tip point and makes the structure fail.

The following points have to be considered due to the above assumption in order to analyze the transmission shaft in ANSYS software.

- Since the LEFM assumption is used, the Stress Intensity Factors, SIFs at a crack tip may be computed using the ANSYS's KCALC command. The analysis used a fit of the

nodal displacements in the vicinity of the crack tip. The shear stress is applied as a remote stress to the infinitesimal part of the transmission shaft.

- Due to the symmetry of the problem, only a quarter part of it is modeled and analyzed. So the boundary condition for the model is a symmetry boundary condition at the left and bottom side.
- The crack-tip region is meshed using quarter point (singular) 8-node quadrilateral elements to get accurate results. The meshed quarter part of plate with central crack is shown in figure 5-6.

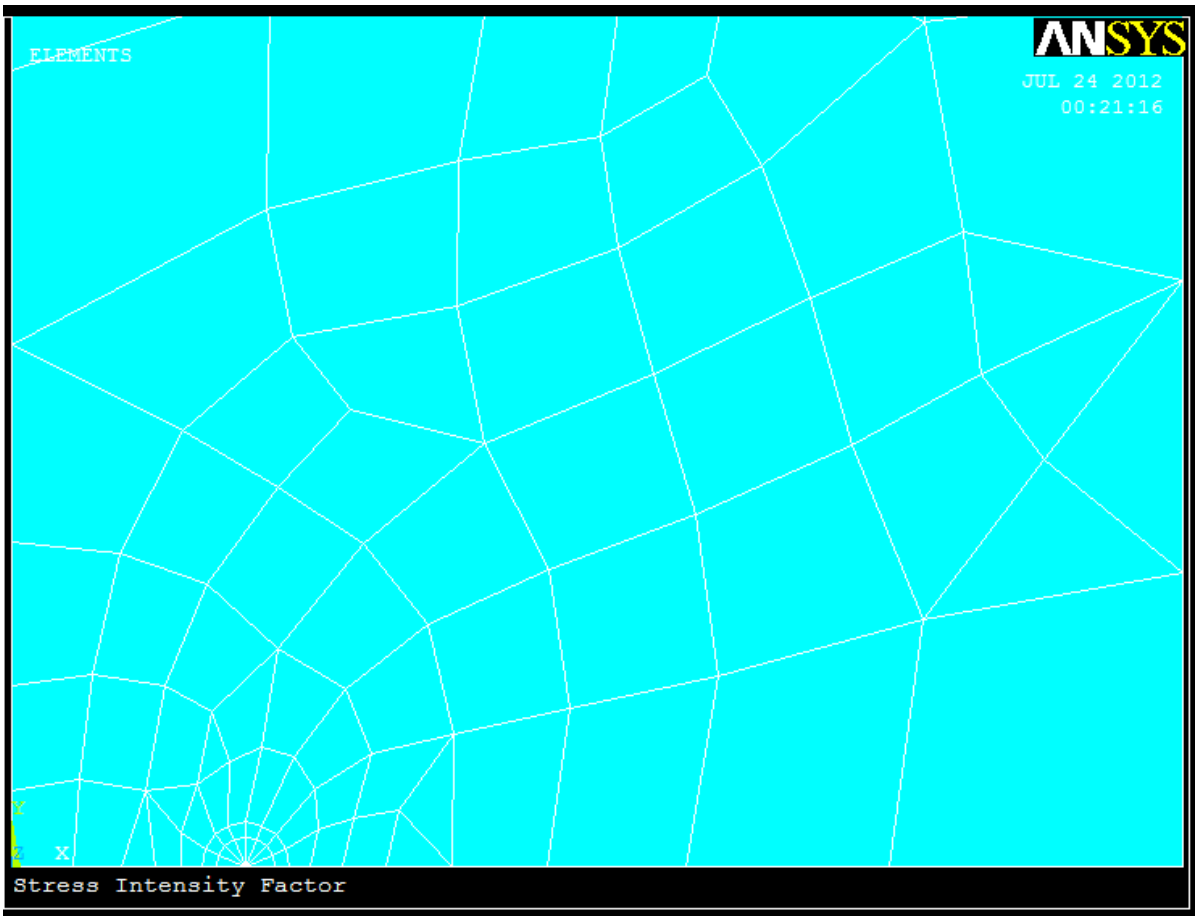

Figure 5-6: - Meshed quarter part of plate with central crack

The deformed shape of the infinitesimal plate is shown in figure 5-7. The stress intensity factor of the plate is obtained and shown in figure 5-8. This figure is taken from ANSYS word pad text as a picture.

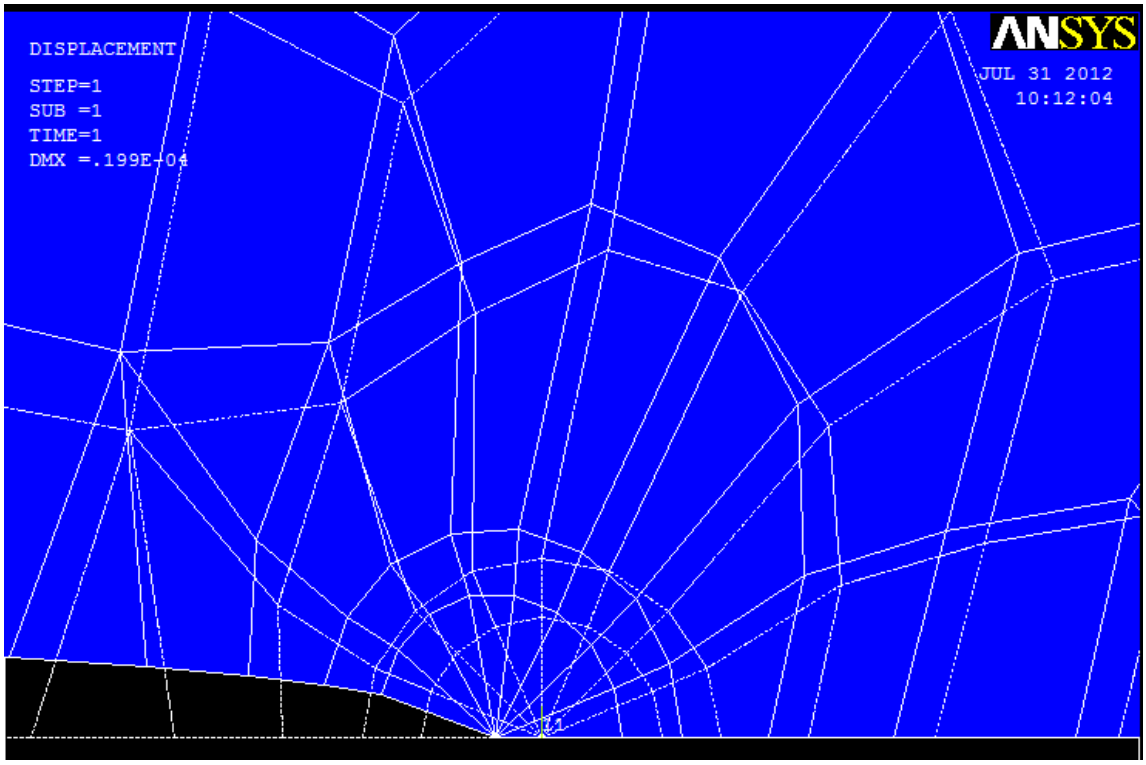

Figure 5-7: - Deformation of the central symmetry crack

```
****  CALCULATE MIXED-MODE STRESS INTENSITY  FACTORS  ****

  ASSUME PLANE STRAIN CONDITIONS

  ASSUME A HALF-CRACK MODEL WITH SYMMETRY BOUNDARY CONDITIONS (USE 3 NODES)

  EXTRAPOLATION PATH IS DEFINED BY NODES:        2      15      14
   WITH NODE       2 AS THE CRACK-TIP NODE

  USE MATERIAL PROPERTIES FOR MATERIAL NUMBER     1
   EX =    0.38000E+06   NUXY =    0.32000      AT TEMP =  0.0000

****  KI =   19.901     ,   KII =   0.0000    ,   KIII =   0.0000      ****
```

Figure 5-8: - Stress intensity factor from ANSYS

The maximum stress is at the crack tip since there is a stress concentration at sharp edges. The Von Misses stress from ANSYS also reveals this fact as shown in figure 5-9.

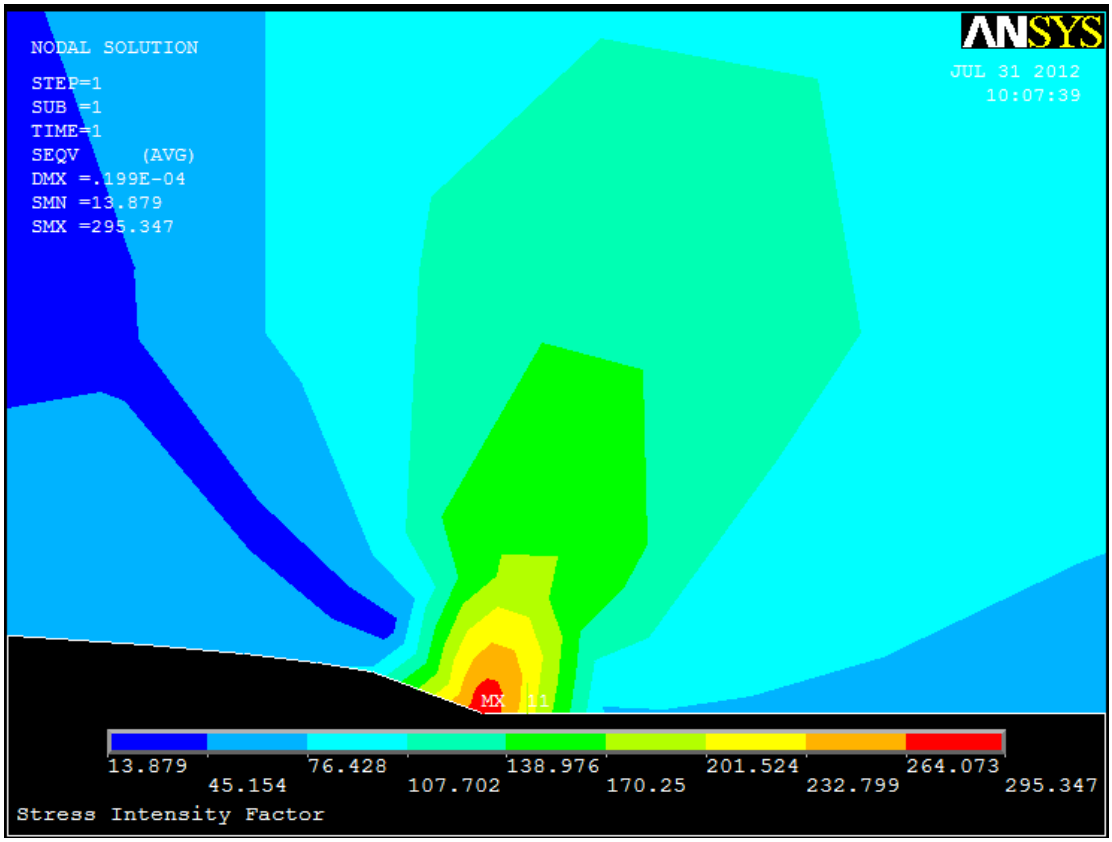

Figure 5-9: - Von Misses stress of the cracked plate

6. Solution Techniques

6.1. Introduction

The analytical analysis of torque capacity and crack propagation of the transmission shaft is done based on the theories of crack on rotating shaft. The rotating glass fiber-reinforced polyester polymer hollow transmission shaft is also analyzed using finite element analysis software by modeling it on ANSYS. The torque capacity of the transmission shaft is also analyzed on ANSYS software until its maximum shear stress becomes equal to the yielding shear stress of the fiber-polyester composites. The torque capacity of the fiber-reinforced composite hollow shaft is also tested on torsional testing machine. The experimental data obtained from the testing machine is collected using the format in Appendix-B. Finally, the results obtained from the analytical analysis and ANSYS software are compared. Similarly, the torque capacities of the transmission shaft obtained from ANSYS and from the testing machine are compared.

6.2. Testing

Testing of the hollow transmission shaft is necessary. In order to perform this task a testing machine has to be set up in the way it gives the required results. A torsional testing machine from Defense Engineering College was used for testing of the shaft. The hollow transmission shaft specimen was tested in testing machine for how much torque it can hold.

The experiment outlines the proper procedure for determining the torque capacity of glass fiber-reinforced hollow circular composite shaft. During this experiment different ply-angle orientation and thickness of the hollow shaft were used as samples to demonstrate how torque capacity changes due to change in thickness and varying angle-ply orientation. By rotating the handle of the testing machine to increase the twisting angle of the shaft, torque was read on the digital torque indicator for different samples. Ultimately, the maximum torque capacity of the glass fiber-reinforced hollow composite shaft was determined. Numerically, the torque can be

calculated using equation (6.1) if the shear module, twisting angle, and dimension of the shaft are known.

$$T = \frac{G\varphi J}{L} \quad \text{.....(6.1)}$$

Where T is the torque applied, G is shear modulus of the fiber-polyester composite, L is the length of the specimen, φ is the angle of twist in radian, J is the polar moment of inertia.

The polar moment of inertia of the specimen is expressed as follows:

$$J = \frac{\pi}{2}\left(R^4 - r^4\right) = \frac{\pi}{32}\left(D^4 - d^4\right) \quad \text{.....(6.2)}$$

R and D are the outside radius and diameter, and r and d are the inside radius and diameter of the cross-sectional test area of the glass fiber-reinforced composite hollow shaft respectively. It is possible to know how much shear stress, τ will be produced on the shaft when it is subjected to the torque above using the following relationship.

$$\tau = \frac{Tr}{J} \quad \text{.....(6.3)}$$

The apparatus used for this experiment measures the angle of twist in degrees rather than in radians. So the shear strain, γ produced by the torque applied is obtained using equation (6.4).

$$\gamma = \frac{\pi r \varphi}{180L} \quad \text{.....(6.4)}$$

Where, φ is the twisting angle in degrees and L is the length of the shaft.

Equipments and testing procedure

The equipments used in this experiment are:

1. Torsion testing machine: - It is a machine used for performing the experiment. It has digital torque gauge, rotation arm, rotating balancing arm and two hexagonal head that are used to cling the specimen. It has the capacity to measure only up to 160Nm torque. The testing machine was setup to hold a specimen of length 200mm and a hexagonal head of flat length 17mm. The testing machine is shown in figure 6-1.

Figure 6-1: - Torsion testing machine

2. Specimen: - It is a glass fiber-reinforced polyester polymer composite hollow circular transmission shaft specimen manufactured in Dejen Aviation Engineering Complex with different orientation angles, stacking sequence and thickness. The specimens are shown in figure 6-2. The different specimens used for this experiment has different thickness, stacking sequence and angle orientation as shown in table 6-1.

Figure 6-2: - Glass fiber-reinforced hollow circular shaft specimens

Table 6-1: - Specimens of different size and angle of orientation

S/N	Specimen nomenclature	Internal diameter [mm]	External diameter [mm]	Thickness [mm]
1	$[90]_2$	18	20	1
2	$[90]_4$	16	20	2
3	$[90]_6$	14	20	3
4	$[+45/-45]_1$	18	20	1
5	$[+45/-45]_2$	16	20	2
6	$[+45/-45]_3$	14	20	3
7	$[+45/90/-45]_1$	18	20	1
8	$[+45/90/-45]_2$	16	20	2
9	$[+45/90/-45]_3$	14	20	3

3. End clamping steel: - It is a structure which has hexagonal head at one end to be inserted into the testing machine cavity and hollow cylinder at the other end to clamp the end of the specimen. The cylinder end of clamping steel has four gaps longitudinally up to the base of the cylinder. This made it to have a spring property to clamp the specimen. This structure is shown in figure 6-3.

4. Hose clip: - This uses to clamp the end clamping steel and the specimen together. The assembled specimen with its end steel clamp and hose clip is shown in figure 6-3.

Figure 6-3: - Assembled specimen, end clamp and hose clip together

The assembled specimen should be secured in the torsion testing machine with its hexagonal end inserted to the hexagonal head of the machine as shown in figure 6-4. The control used to generate twisting can be used to balance the arm and torque gage. When the apparatus is set to read zero degrees twist and torque, the angle of twist can be induced. While the digital torque reader is set to be zero, the compensation wheel should set the compensation to zero.

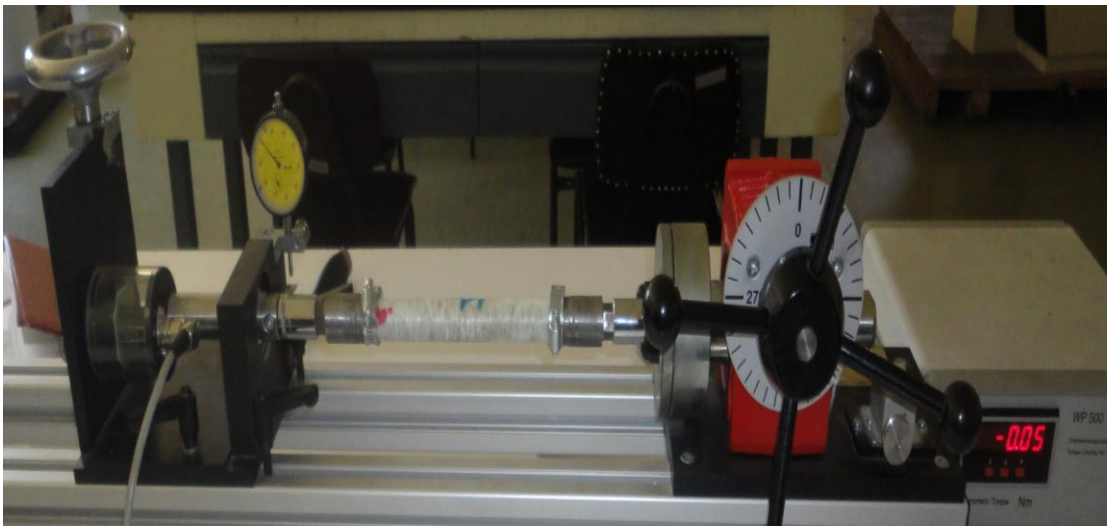

Figure 6-4: - Torsion testing machine with specimen

The procedures to test the torque capacity of the transmission shaft are described as follows:

- Twist is induced in quarter degree increments. After each application, the arm should be balanced and the resulting torque recorded.
- When 8 degrees of twist has been applied, the twist should be increased in 2 degree increments. Again, the arm should be balanced after each step. Record the torque and record if any hysteresis effects are experienced.
- After 30 degrees of twist has been applied, the twist should be increased first to a total twist of 90 degrees. Record the torque and note any hysteresis effects. Next, increment the angle of twist in 90 degree increments until the specimen breaks. After every increment, record the torque. Usually this process needs to be done fairly quickly to ensure minimal error due to relaxation in the specimen.

7. Result and Discussion

The mass of the carbon steel 6061 transmission shaft of the helicopter is 10kg whereas the mass of the glass fiber-reinforced polyester polymer composite hollow transmission shaft is 6.5kg. Therefore, the mass of the transmission shaft decreases by 35%, which is important for the helicopter to reduce its weight.

The maximum shear stress developed due to the applied torque on the transmission shaft is 75MPa, which is very small to cause failure. Even the stress at the crack tip is 287MPa which is less than yielding stress of the glass fiber-polyester resin composite material.

The torque capacity of the fiber-reinforced composite transmission shaft has enough capacity to carry the torque that was produced by the engine of the helicopter. The torsional buckling capacity of the fiber-reinforced transmission shaft is less than the critical torsion buckling capacity of the composite transmission shaft.

The result obtained from ANSYS also shows that as the thickness of the glass fiber-reinforced polyester polymer composite hollow transmission shaft increases the stress decreases. When the stacking sequence varies the stress developed due to the applied torque also varies. This indicates that the torque capacity of the transmission shaft increases as its thickness increases; its torque capacity also varies as the stacking sequence varies. The results obtained from ANSYS are plotted as shown in figure 7-1.

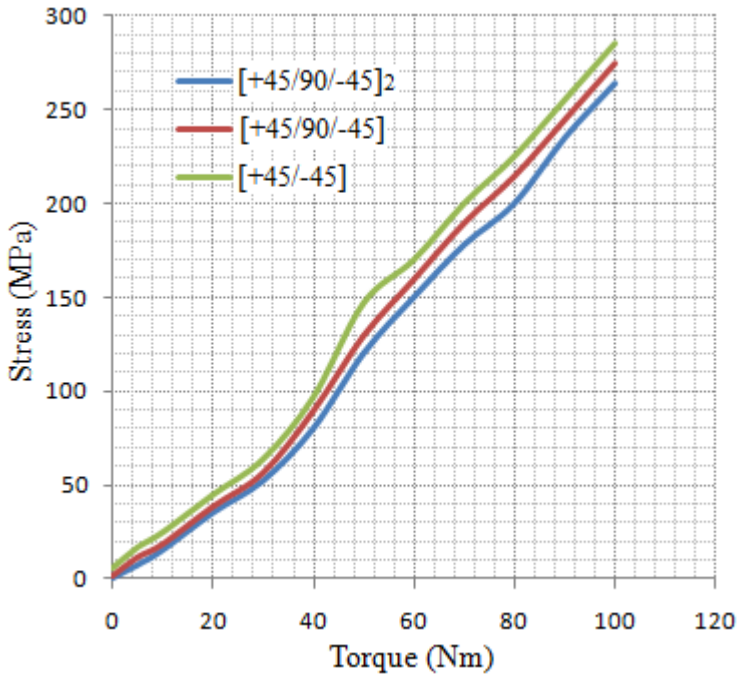

Figure 7-1: - Torque versus stress $[+45/90/-45]_2$, $[+45/90/-45]$ and $[+45/-45]$

It is also possible to plot the results obtained from ANSYS in torque versus twisting angle by changing the stress into twisting angle by using the relation between twisting angle and stress. The graph shown in figure 7-2 indicates that the torque varies with thickness, orientation angle and stacking sequence of the glass fiber-reinforced polyester polymer composite hollow transmission shaft in ANSYS.

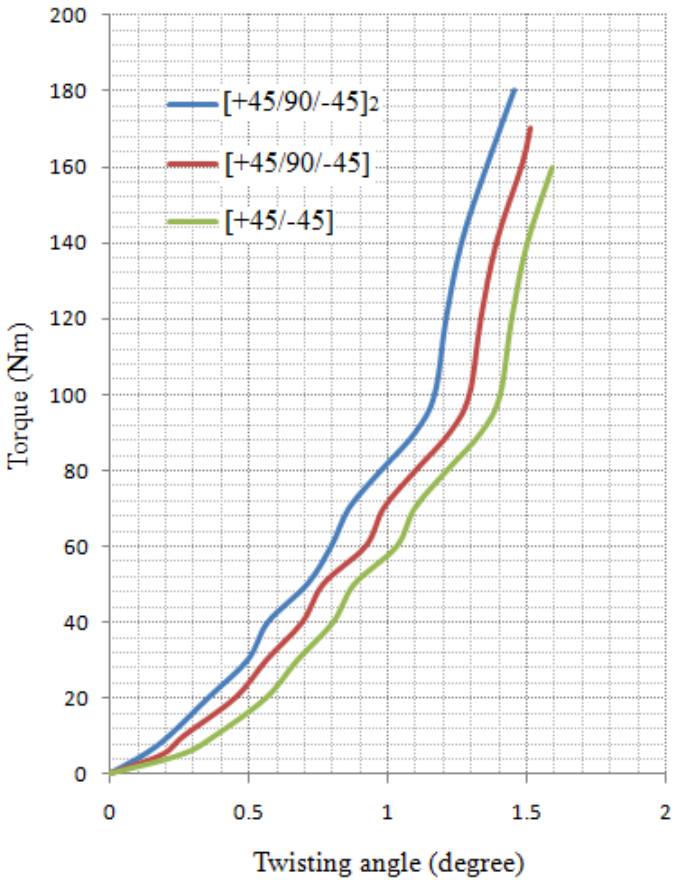

Figure 7-2: - Torque vs twisting angle $[+45/90/-45]_2$, $[+45/90/-45]$ and $[+45/-45]$

The testing results of the transmission shaft are consistent to the finite element method results and numerical results. A four pieces of each specimen has been tested and the torque on the digital torque recorder was recorded step by step while the wheel was rotating at constant speed continuously. The torques were recorded first at one forth of a revolution, second at three fourth of a revolution, third at five fourth of a revolution, and finally at each end of one full revolution.

The testing results for a thickness of 1mm, 2mm and 3mm and orientation angle 90^0 is depicted in figure 7-3. As sown in the figure, the torque capacity of glass fiber-reinforced polyester polymer composite hollow shaft increases as its thickness increases.

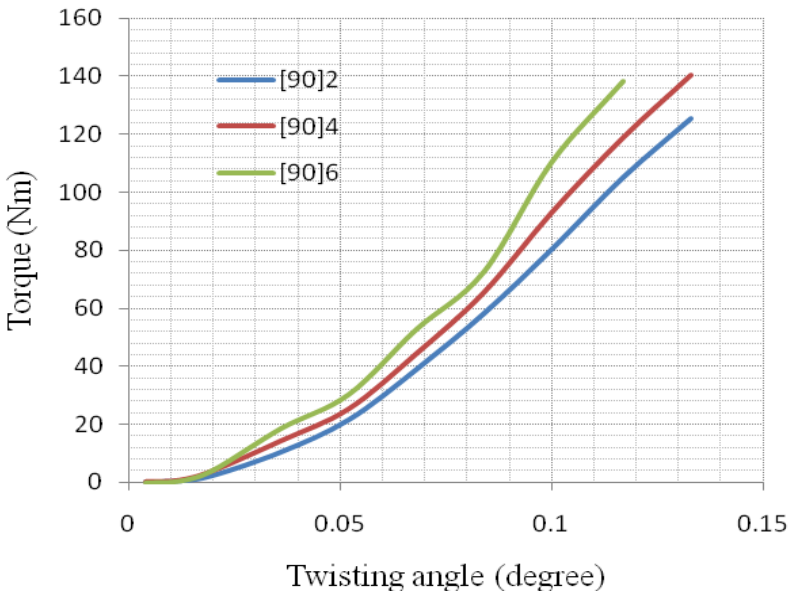

Figure 7-3: - Torque versus twisting angle for $[90]_2$, $[90]_4$ and $[90]_6$

The testing result for thicknesses of 1mm, 2mm and 3mm and orientation angle of 45^0 is shown in figure 7-4. The torque capacity of the glass fiber-reinforced polyester polymer composite shaft increases as its thickness increases.

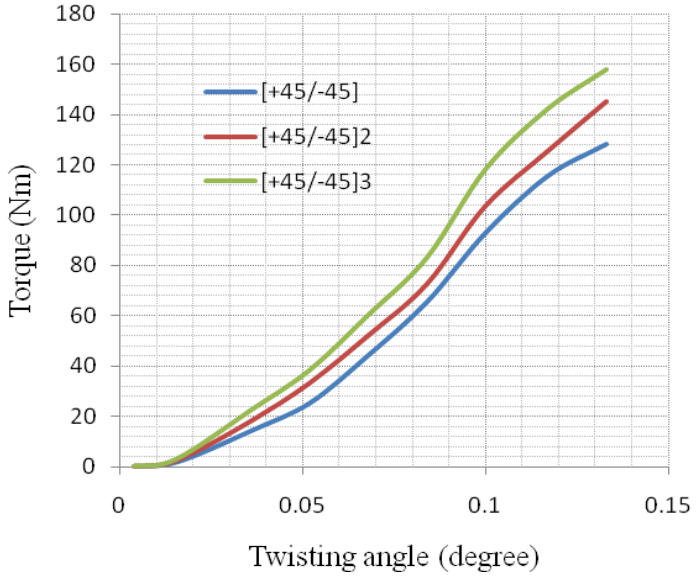

Figure 7-4: - Torque versus twisting angle for $[\pm 45]$, $[\pm 45]_2$ and $[\pm 45]_3$

The testing result for thickness of 1mm, 2mm and 3mm and combined orientation angle of 90^0 and 45^0 with stacking sequence shown is depicted in figure 7-5. The torque capacity of the glass fiber-reinforced polyester polymer composite shaft increases as its thickness increases and varies as the stacking sequences varies.

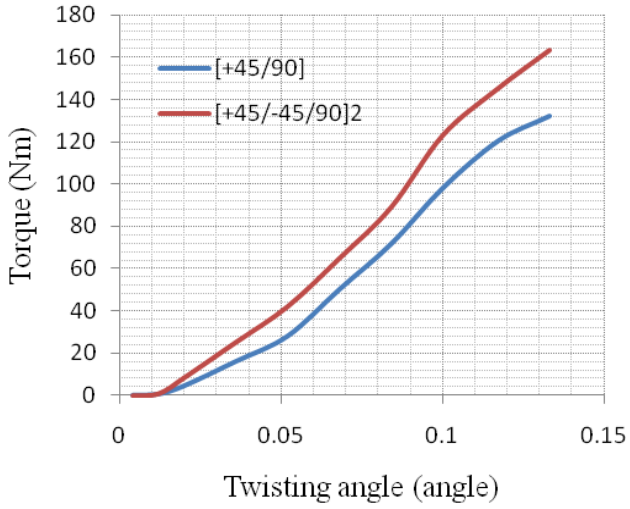

Figure 7-5: - Torque versus twisting angle for $[+45/90]$and $[\pm 45/90]_2$

The torque of the glass fiber-reinforced polyester polymer composite transmission shaft varies with the variation of the stacking sequence even though the thickness is constant. As shown in figure 7-6 the stacking sequence of [+45/90] has better torque capacity than the stacking sequence of [+45/-45] and $[90]_2$.

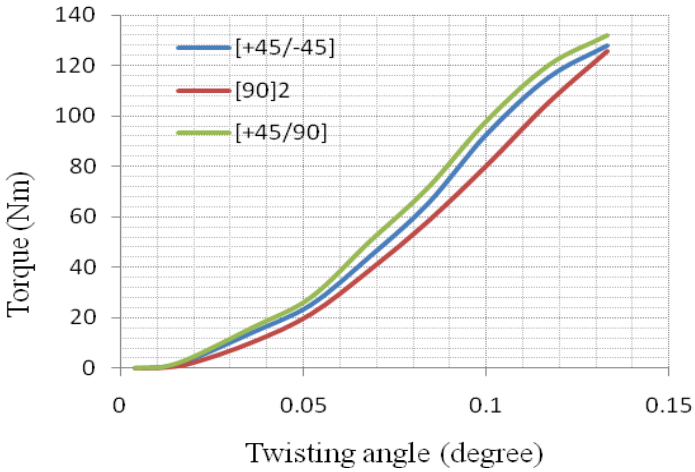

Figure 7-6: - Torque versus twisting angle for $[\pm 45]$, $[90]_2$ and $[+45/90]$

In figure 7-7 the torque increases when the thickness increases. The $[+45/-45/90]_2$ stacking sequence is still better than the $[+45/-45]_3$ and $[90]_6$ stacking sequence.

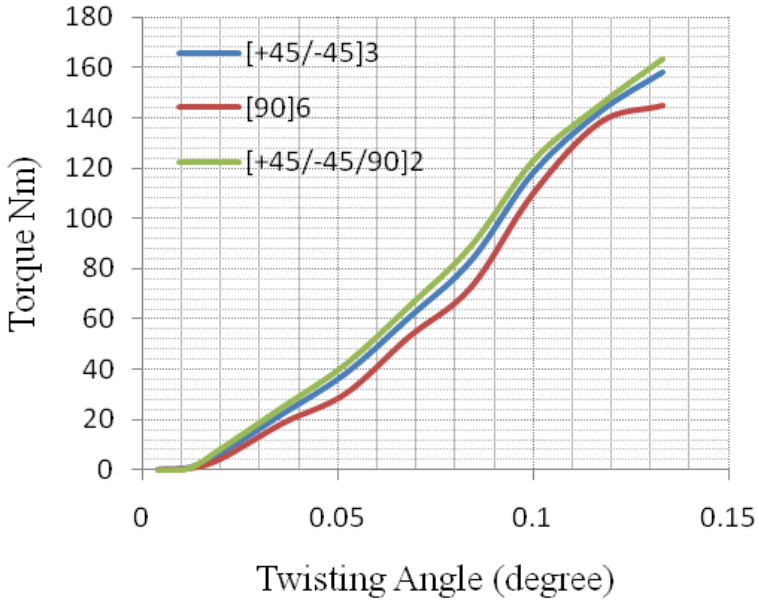

Figure 7-7: - Torque versus twisting angle for $[\pm 45]_3$, $[90]_6$ and $[\pm 45/90]_2$

It is clear from the above figures that $[+45^0/-45^0/90^0]_{2s}$ stacking sequence and a six number of layers has better torque capacity than the others. So this stacking sequence and number of layers is selected for the transmission shaft of the helicopter. The ANSYS and experimental results from the above shows have also similar output.

So now it is possible to compare the results obtained from the experiment and ANSYS. The torque capacity of the glass fiber-reinforced polyester polymer composite hollow transmission shaft increases with thickness and varies with orientation angle and stacking sequence both in ANSYS and experimental results as shown in figure 7-8.

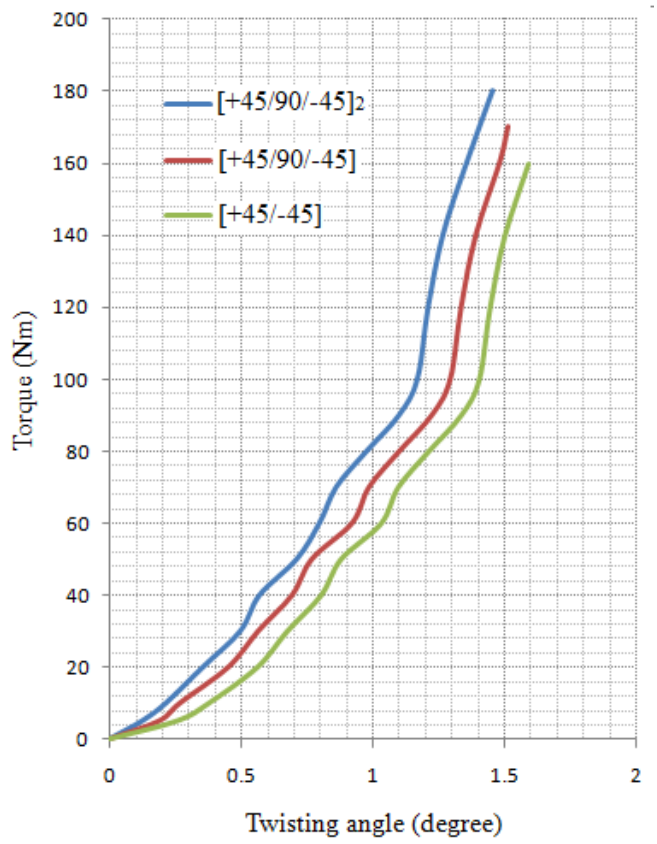

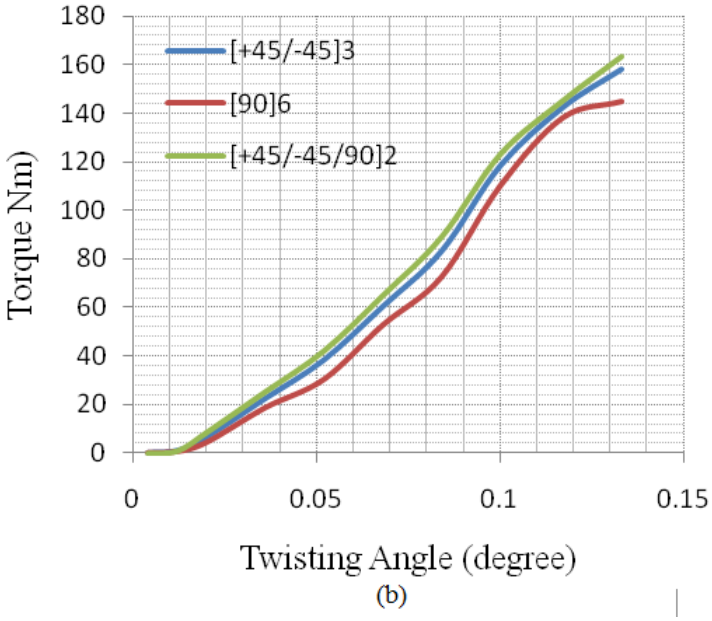

Figure 7-8: - Comparison between the (a) ANSYS and (b) experimental results

Chapter Eight

8. Conclusions and Recommendations

8.1. Conclusions

Fiber-reinforced composites offer many advantages compared to conventional materials such as metals. Their light weight provides a tremendous advantage in terms of strength-to-weight ratio. Since a broken fiber limits the crack size and crack extension, the chance of reaching the critical crack size is slim, even when bundles of nearby fibers are cracked. So in terms of fracture mechanics, fiber-reinforced materials have a good resistance to crack propagation. However, fiber-reinforced composites are highly susceptible to moisture and temperature. Their mechanical and physical properties consequently decrease to various degrees in such environments.

In this study, the torque capacity and crack propagation of the glass fiber-reinforced polyester polymer composite transmission shaft were analyzed through finite element analysis software, ANSYS. The thickness of the glass fiber composite transmission shaft was determined by considering the applied torque on it. The advantage of using this fiber-reinforced composite material for the transmission shaft helps to reduce its mass by keeping its strength as carbon steel 6061.

In this thesis, the torque capacity, crack propagation and torsional buckling capacity were also analyzed analytically. From the analysis results, it can be seen that the glass fiber-reinforced polyester polymer composite transmission shaft has good crack extension resistance and is capable to carry the torque applied from the engine of the helicopter.

Torsion testing for torque capacity was carried out for glass fiber-reinforced polyester polymer composite hollow transmission shaft. An experiment was done for four laminate types with different orientation angles, stacking sequences and number of layers. The conclusions made from this experiment are summarized as follows:

- ❖ Increasing the number of layers i.e. the thickness would increase the torque capacity of the glass fiber-reinforced polyester polymer composite hollow transmission shaft.
- ❖ There was no glass fiber breakage observed from the composite hollow transmission shaft tests, even when the delamination takes place. This phenomenon took place only in low load torsion test. But, at high load catastrophic failure occurred for the glass fiber-reinforced polyester polymer composite hollow transmission shaft.
- ❖ Changing the stacking sequence and orientation angle of composite laminate of the transmission shaft changes its torque capacity. Combing orientation angle in winding the composite laminate of the transmission shaft also enhances its torque capacity.
- ❖ Glass Fiber-reinforced polyester polymer composite hollow transmission shaft with laminates of $[+45^0/-45^0/90^0]_{2s}$ stacking sequence has the highest torque capacity.

Finally, the safety of the designed glass fiber-reinforced polyester polymer composite hollow transmission shaft was evaluated by considering the results obtained analytically, numerically and experimentally, which they have good agreement.

8.2. Recommendations for future researches

In this research, the torque capacity and the crack propagation of the glass fiber-reinforced polyester polymer composite material is studied. Even though it is expensive, carbon fiber has better mechanical and physical properties than glass fiber. So if carbon fiber is used it will be much better. I can also recommend carbon fiber for the transmission shaft of the H260L model helicopter. Epoxy resin is also recommended instead of polyester resin.

In order to be sure that the fiber-reinforced composite transmission shaft is better than the monolithic material, which is steel, the research which is done on this paper is not enough. Further study on the fiber-reinforced polymer composite material is necessary. Since there is high heat generation during the rotation of the transmission shaft of the helicopter, doing research on thermal property of the fiber-reinforced polymer composite transmission shaft is important.

As far as there are rotating parts in operation, there is a shock and vibration. So vibration analysis on the fiber-reinforced polymer composite transmission shaft of the helicopter is also necessary.

So I recommend further study on the aforementioned two points by respective researchers. After researches on the thermal and vibration analysis is done and gets it safe, it is advantageous to change the steel transmission shaft of the Hidasie helicopter with the glass fiber-reinforced polyester polymer composite transmission shaft.

References

1. D. Hull, 1995, An introduction to composite materials, Cambridge University press
2. Valery V. Vasiliev & Evgeny V. Morozov, 2007, Advanced Mechanics of composite materials, Second edition, Elsevier Ltd.
3. Murat Kisa, 2003, "Free vibration analysis of a cantilever composite beam with multiple cracks", *Composites Science and Technology* 64 (2004) 1391-1402
4. Murat Kisa, M. Arif Gurel, 2007, "Free vibration of uniform and stepped cracked beams with circular cross sections", *International Journal of Engineering Science* 45 (2007) 364-380
5. Li Jun, Hua Hongxing, Shen Hongxing, Shen Rongying, 2007, "Dynamic stiffness analysis for free vibrations of axially loaded laminated composite beams", *composite structure* 84 (2008) 87-98
6. S.K. Bhaumik, R. Rangaraju, M.A. Venkataswamy, T.A. Bhaskaran, R.V. Krishnan, 2002, "Fatigue failure of a hollow power transmission shaft", *Engineering Failure analysis*, 9 (2002) 457-467
7. H.S. Kim, D,G, Lee, 2004, "Optimal design of the press fit joint for a hybrid aluminum/composite drive shaft", *composite structures*, 70 (2005) 33-47
8. Y.A. Khalid, S.A. Mutasher, B,V, Sahari, A.M.S, Hamouda, 2004, "Bending fatigue behavior of hybrid aluminum/composite drive shafts", *Material and design*, 28 (2007) 329-334
9. C. Y. Chang, M. Y. Chang, J. H. Huang, 2004, "Vibration analysis of rotating composite shafts containing randomly oriented reinforcements", *Composite structures*, 63 (2004) 21-32
10. K.G. Bang, D.G. Lee, 2002, "Design of carbon fiber composite shafts for high speed air spindles", *Composite structures*, 55 (2002) 247-259
11. S.A. Mutasher, 2008, "Prediction of torsional strength of the hybrid aluminum/composite drive shaft", *Material and Design*, 30 (2009) 215-220
12. G. Sanjay, A.J. Kumar, 2007, "Optimum design and analysis of a composite drive shaft for an automobile", *Blekinge Institute of Technology Karlskrona,* Sweden

13. R.B. Ingle and B.B. Ahuja, 2005, “An experimental investigation on performance characteristics and natural frequency analysis of high-speed carbon-epoxy shaft in aerostatic conical journal bearing”, *Journal of Scientific and Industrial Research*, 64(2005)571-580

14. Guillermo A. Riveros, 2006, “Numerical Evaluation of Stress Intensity Factors (KI) J-Integral Approach”, *US Army Corps of Engineers*, ERDC/CHL CHETN-IX-16

15. D.J. Bieryla, M.W. Trethewey, C.J. Lissenden, M.S. Lebold, and K.P. Maynard, 2005, “Shaft Crack Monitoring via Torsional Vibration Analysis”, Part one laboratory test
16. J.R. Vinson, R.L. Sierakowski, 2007, The behavior of structures composed of composite materials, Elsevier Ltd
17. Valery V. Vasiliev, and Evgeny V. Morozov, 2007, Advanced mechanics of composite materials, Elsevier Ltd
18. F L Matthews, G A O Davies, D Hitchings and C Soutis, 2003, Finite element modeling of composite materials and structures, first edition, Woodhead publishing Ltd. and CRC press LLC
19. Frederick T. Wallenberger, and Paul A. Bingham, 2010, Fiberglass and glass technology *Energy-friendly compositions and applications*, Springer Science+Business Media LLC
20. Instruction and flight manual for model H260LL Helicopter, Publication Number: VA4045-10, 2010
21. Dr. Markus Milwich, 2009, Faserverbundwerkstoffe handbuch/Composite materials handbook, sixth edition, ITV Denkendorf
22. Y. Nakasone, S. Yoshimota and T.A. Stolarski, 2006, Engineering analysis with ANSYS software, first edition, Elsevier Ltd
23. Robert L. Norton, 2006, Machine Design an Integrated Approach, third edition, Pearson Education Inc.

24. Arthur P. Boresi and Richard J. Schmidt, 2003, Advanced Mechanics of Materials, sixth edition, John Wiley & Sons, Inc.
25. S. Timoshenko and J. N. Goodier, 1951, Theory of Elasticity, second edition, McGraw-Hill Book Company, Inc.
26. P. R. Baviskar and V. B. Tungikar, 2011, "Analysis of crack in shaft of blower using finite element analysis and experimental technique", *IJRRAS 8(1),* Vo18Issue1-8-1-05
27. Alun F. Liu, 2005, Mechanics and Mechanisms of Fracture: An Introduction, first edition, ASM International, USA
28. S.P. Timoshenko and J.M. Gere,1985, Theory of elastic stability, second edition, McGraw-Hill International Book Company, New York
29. Stephen R. Swanson, 1997, Introduction to design and analysis with advanced composite materials, Prentice-Hall International, Inc.
30. S.S. Rao, 2002, Mechanical Vibrations, second edition, Addision-Wesely Publishing Company
31. Lim.J.W. et.al, 1986, "Optimum sizing of composite power transmission shafting", *Journal of American Helicopter Society*, Vol.31, No.1
32. T. L. Anderson, 1994, Fracture Mechanics: Fundamental and Applications, second edition, CRC press
33. M. Janssen, J. Zuidema and R. J. H. Wanhill, 2004, Fracture Mechanics, second edition, Spon Press, New York
34. E.E. Gdoutos, 2005, Fracture Mechanics: An Introduction, second edition, Springer
35. Nestor Perez, 2004, Fracture Mechanics, first edition, Kluwer Academic Publishers
36. ANSYS 12.0 Classic software help inbuilt tutorials for structural analysis

Appendix-A

The mechanical property of the glass fiber-reinforced polyester polymer composite transmission shaft is obtained using the following MATLAB code.

```
function [Ex,Ey,Gxy,vxy,vyx]=eng_const(E1,E2,G12,v12)
phi=0.65;     %input('enter the volume fraction of fiber: ')
Ef=73;        %input('Enter the Youngs modulus of glass fiber: ')
Em=3.5;       %input('Enter the Youngs modulus of polyester resin: ')
E1=phi.*Ef+(1-phi).*Em;
E2=(Em.*Ef)/(phi.*Em+(1-phi).*Ef);
vf=0.18;       %input('Enter the poissons raio of glass fiber: ')
vm=0.26;       %input('Enter the poissons ratio of polyester: ')
v12=phi.*vf+(1-phi).*vm;
Emm=Em./(1-vm^2);
E22=(Emm.*(1-0.85*phi^2))./(((phi.*Emm)./Ef)+(1-phi)^1.25);
Gf=30.9;      %input('Enter the shear modulus of glass fiber: ')
Gm=0.59;      %input('Enter the shear modulus of polyester resin: ')
G12=(Gm.*Gf)./(phi.*Gm+(1-phi)*Gf);
G22=(Gm.*(1+0.6.*phi^0.5))/((phi.*Gm)./Gf+(1-phi)^1.25);
Qsks=[E1./1-(v12.*E2)./E1 (v12.*E1)./1-(v12.*E2)./E1 0;...
    (v12.*E1)./1-(v12.*E2)./E1 E1./1-(v12.*E2)./E1 0;0 0 G12];
angle=input('Enter the angle orientation it forms: ');
theta=(angle.*pi)./180;
T=[(cos(theta))^2 (sin(theta))^2 2*sin(theta)*cos(theta);...
    (sin(theta))^2 (cos(theta))^2 -2*sin(theta)*cos(theta);...
    -sin(theta)*cos(theta) sin(theta)*cos(theta)...
    (cos(theta))^2-(sin(theta))^2];
Qlam=T*Qsks*T';
tk=0.5;     %input('Enter the ply thickness: ')
t=input('Enter the thickness: ');
n=input('Enter the number of layers: ');
A=(n.*tk./t).*Qlam;
a=inv(A);
Ex=1./a(1,1);
Ey=1./a(2,2);
Gxy=1./a(3,3);
vxy=a(2,1)./a(1,1);
vyx=a(1,2)./a(2,2);
num=1:1:5;
eng_cons=[Ex;Ey;Gxy;vxy;vyx];
result=[num' eng_cons]
end
```

Appendix-B

Work sheet for torsional test

Glass fiber-reinforced Hollow shaft dimension

L = _____ Millimeter (test length)

d_0 = _____ Millimeter (specimen outside diameter)

t = _____ Millimeter (thickness)

α = _____ Degrees (fiber orientation angles)

Test number_____

Test Data

Angle of twist, φ (degrees)	Torque read by the digital torque reader, T (Nm)

Declaration

I am hereby to declare that this thesis work is my original work and has not been presented for a degree in any other university, and that all source of materials are duly acknowledged.

Name: Okqubamariam Leake

Signature: _____

Thesis Title: *Torque Capacity and Crack Propagation Analysis of Fiber-reinforced Composite Hollow Transmission Shaft*

Department: ___Dr. Daniel Tilahun____

Signature: _____

Advisor: _Professor Eyassu Woldesenbet

Signature: _____